NTNU – Trondheim
Norwegian University of
Science and Technology

Model of Hook Load During Tripping Operation

Edvin Kristensen

Petroleum Geoscience and Engineering
Submission date: June 2013
Supervisor: Pål Skalle, IPT

Norwegian University of Science and Technology
Department of Petroleum Engineering and Applied Geophysics

Acknowledgements

This report has consumed many working hours for the author, however, it would not have been possible without the kind support from many individuals and organizations.

First I would like to thank my supervisor and Associated Professor at NTNU, Pål Skalle, for his enthusiastic guidance, support and encouraging mood during the thesis work.

My thanks go to Tommy Toverud for our collaboration and for his work in the development of the mathematical model used in this thesis.

Flemming Stene, Kjell Inge Meisal and Statoil deserve gratitude for providing real time drilling data from wells drilled in the North Sea. This has given valuable insight and material for use in the developed model.

Also Ronny Isaachsen, driller in the North Sea, deserves a thank you for giving me explanations and detailed information about field equipment and drilling procedures.

I hereby certify that this work is solely my own.

Trondheim, June, 2013

_____

Edvin Kristensen

Everyone knows a reservoir can`t hang in a well

– Cor J. Kenter

Abstract

Drilling after oil and gas becomes more challenging for every drilled well; deeper, longer, harder, higher temperature, higher pressure and more complex conditions. The equipment requirements and well integrity regulations make the wells increasingly more expensive. The well costs often dominate the total investments for field development. Avoiding trouble while drilling wells constitutes huge potential cost savings.

One way of avoiding trouble is to detect deteriorating conditions in the well and initiate the correct remedies before the trouble evolves. By modeling the physics in the well accurate and detailed, normal well conditions can be defined and deviations from normal will indicate abnormal hole conditions.

The initial goal of this thesis was to understand, investigate and further develop the mathematical model of the weight of the drill string when pulling it out of the hole, presented by Mme et al. (2012). The model was analyzed, evaluated and improvements were initiated. But difficulties arose during the work process and another point of attack had to be selected. An alternative model has therefore been developed and tested against field data supplied by Statoil. The tests gave some affirmative results, but all in all, the alternative model did not manage to match the field measurements in a sufficiently satisfactory manner.

The main conclusion of this thesis work is that to model well conditions accurately, complex and detailed physical models are needed. To model the weight of the drill string when pulling it out of the hole in a sufficient way, the mass – spring model (Mme et al. 2012) has to be further improved and then tested against field cases. The alternative model can be used as a starting point for further development of a tool to detect relative changes of the main forces developing in the well. Another important finding was that to be able to recognize acceleration effects and phenomena happing in a short time interval, sampling frequencies of the field data should be at least 3 Hz. Also it will be beneficial to use field measurements collected consistently at fixed time steps. This would ease and increase the quality of the interpolation.

Sammendrag

Boring etter olje og gass blir mer utfordrende for hver borede brønn; dypere, lengre, hardere, høyere temperatur, høyere trykk og mer kompliserte forhold. Krav til utstyr og brønnintegritet gjør at brønnene blir stadig dyrere. Brønnkostnadene dominerer ofte de totale investeringskostnadene for feltutbygginger. Å unngå problemer under boring utgjør store potensielle kostnadsbesparelser.

En måte å unngå problemer på, er å oppdage de forverrende forhold i brønnen og initiere de riktige prosedyrene før problemene utvikler seg. Ved å modellere de fysiske forholdene i brønnen nøyaktig og detaljert, kan normale brønnforhold defineres og avvik fra normale forhold vil indikere unormale hullforhold.

Det opprinnelige målet med denne oppgaven var å forstå, undersøke og videreutvikle den matematiske modellen av borestrengens vekt under uttrekking ut av hullet, presentert av Mme et al. (2012). Modellen ble analysert, vurdert og forbedringer ble utført. Men vanskeligheter oppsto under arbeidsprosessen og en annen angrepsvinkel måtte velges. En alternativ modell ble derfor utviklet og ble testet mot feltdata levert av Statoil. Testene ga noen bekreftende resultater, men alt i alt, klarte ikke den alternative modellen å matche feltmålingene på en tilstrekkelig god måte.

Hovedkonklusjonen i denne avhandlingen er at å modellere brønnforhold nøyaktig krever komplekse og detaljerte fysiske modeller. For å modellere vekten av borestrengen på en tilstrekkelig måte under uttrekking ut av hullet, så må masse - fjærmodellen forbedres ytterligere, og deretter testes mot feltetdata. Den alternative modellen kan brukes som utgangspunkt for videre utvikling av et verktøy for å detektere relative endringer av de viktigste kreftene i brønnen. Et annet viktig funn var at for å være i stand til å gjenkjenne akselerasjonseffekter og fenomener som utarter seg i et kort tidsintervall, så bør målefrekvensen av feltdataen være minst 3 Hz. Det vil også være fordelaktig å bruke feltmålinger samplet konsekvent på faste tidssteg, samtidig som oppløsningen i tidsdomentet burde være på mer enn hvert hele sekund. Dette vil forenkle og øke kvaliteten på interpolasjonen.

Contents

1 Introduction

The easy oil is gone. Exploring, drilling and producing the remaining oil challenge the existing technology and force the industry to develop better solutions. As oil- and gas wells are increasing both in depth and complexity, the requirements to operational equipment get even more comprehensive. From a drilling point of view, the rig rates and operational costs have reached amounts that make it more interesting than ever to try to reduce the operational downtime; the Non-Productive Time (NPT).

One obvious measure to avoid getting into trouble, and thus reduce the NPT, is to detect potential problems before they occur and take appropriate counter measures. Even though the intention is to drill a smooth and healthy well with constant hole size, mother earth is heterogeneous and changes with time and depth. So do the wells. A well is drilled through several different rock types and formations which all respond differently to changes in stresses and drilling fluids. The hole diameter may increase or decrease due to these changes and operational restrictions may occur. During the drilling operation, restrictions are a major contributor to the NPT and are most often recognized while going into or out of the hole, a drilling activity known as tripping.

Live information from the well during a drilling operation is called Real Time Drilling Data (RTDD). Interpretation of the RTDD gives a picture of the conditions in the well. An important parameter collected is the hook load (HKL). The HKL measurements can be interpreted in trying to understand what is happening down hole. The highest potential of using the HKL measurements in revealing problems occurring in the well is during tripping out or into the well.

The idea of comparing pre-calculated drilling parameters to the measured values to detect abnormal behavior is not new. A technique to determine friction losses in the drill string (DS) on the well site by the use of RTDD was documented in 1989 by Falconer et al. This technique used surface measurements only. Recent development of equipment and data quality has given RTDD a higher potential of revealing deteriorating well conditions, and the mentioned technique was recently automated with success (Niedermayr et al. 2010). The increased automation of the drilling process (, in both hardware and software,) together with the increased quality of the measurement while drilling equipment, giving continues measurements down hole, add two main benefits; comparing surface to downhole values and the continuous plotting of trends. The deviations between measured values and the output values of a trustworthy model

can be said to be abnormal, or possibly indicate poor hole conditions which indicate that counter measures ought to be taken.

A big challenge of the theoretical modeling is to take into account all the different parameters and effects that happen downhole and give output values that match the experienced ones. Cayeux et al. (2012a) stated that physical calculations in most cases provide estimates which are not even close to the measured ones (!). This is caused by the uncertainty in some of the key input parameters and the mentioned paper points out the critical need for accurate calibration during operation.

Cordoso et al. (1995) pointed out that most of the directional well drilling problems occur during tripping operations. The long term goal of this report is to be able to better detect and reveal abnormal downhole behavior during tripping operations. Ideal and good hole conditions will be identified in RTDD and normal hole conditions will be tried modeled by mathematical equations. This way, the model's validity and reliability can be checked and hopefully verified. The value of this work is that if the model is trustworthy, any deviations from the model output could indicate trouble and poor conditions down hole. The work in this thesis is based on, and is a continuation of, the project thesis "Field and Experimental Investigation of Hook Load" (Kristensen 2013). The mass – spring model presented in Mme et al. (2012) will be investigated and a new model will be presented.

To reach the mentioned goals, this report will;

- Describe the theory and history of HLK measurements
- Explain what influences the measured weight of the drill string
- Detect and present the physical effects that influence friction
- Present history of well friction modeling and practical applications
- Give examples of typical development of HKL during the pulling of one stand
- Explain the structure and idea behind the mass – spring model and the new alternative model
- Present the RTDD used for simulations
- Present results
- Discuss and evaluate results, models and RTDD
- Give a conclusion of the thesis work and give recommendations of further work

2 Hook Load Theory

This chapter is based on material and work done in relation to the project thesis (Kristensen 2013), written by the author of this report. The chapter will give an introduction to the term hook load (HKL) and explain how the physics of the involved forces are working. These basics will be needed in order to understand the concept of well friction and the mathematical models of HKL during tripping operations that will be presented later on.

2.1 Definition

There are many ways of defining the suspended weight in the hook (denoted W in Fig. 1). Mme et al. (2012) defines it as "sum of vertical components of the forces acting on the drill string attached to the hook", and Schlumberger (2012) as; "total force includes the weight of the drill string in air, the drill collars and any ancillary equipment, reduced by any force that tends to change that weight".

The weight of the pipes and equipment that make up the drill string are known at surface conditions before it goes down into the hole. As the hole starts digging, circulation is established and the drill string feels a buoyant uplifting force. The well increases in depth and it might deviate from the vertical direction, resulting in friction forces against the wellbore walls. The wellbore stability could be poor and parts of the formation might fall into the well. High fluid circulation rates of drilling fluid might be needed to maintain sufficient cleaning capacity.

These are examples of typical scenarios that might occur while drilling a well. The next subchapters will define the different forces and how they affect the experienced and measured HKL.

2.2 Rig Set Up – HKL Sensor

The use of sensors and instruments were relatively early adapted and implemented to drilling operations. The first patent of a weight indicator for the load suspended in the hook was issued as early as in 1906 to John Sharpe. Despite the increase in use of electronic sensors today, the Martin-Decker diaphragm-type weight indicator developed in 1926 still remains one of the most commonly used types (Schooley 2008). The diaphragm type sensor is a closed hydraulic system with gauge

pressure indicator. This type of sensor has its limitations and weaknesses that should be understood and taken into account, if used as an input parameter to a model (Florence and Iversen 2010). The equipment used in the drilling industry is a combination of new and old. Today the newest types of hoisting equipment on a rig often have several electronic measurements in the system, often in the Draw Works and in the Travelling Block[1] (see Fig. 1). Due to this blend of different equipment, it is important to know the method used for measuring the parameter of interest in order to be aware of its limitations.

A conventional mast (derrick) and drill floor set-up, with respect to hoisting and lowering of the drill string, is shown in Fig. 1. In this configuration, the weight suspended in the hook is a function of the tension in the Dead Line, measured by the Load Indicator. Other derrick systems and ways of measuring the weight also exist, but the configuration described here illustrates the principles and makes it easily understood.

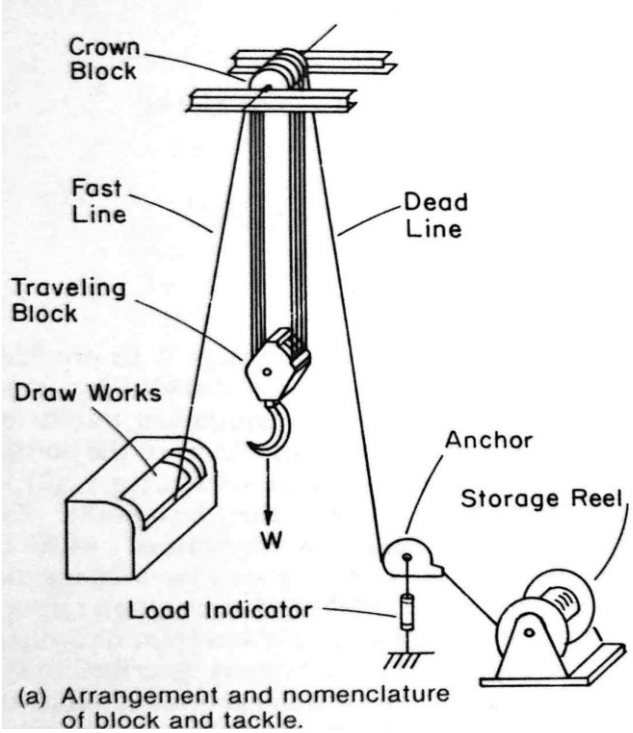

Figure 1: The figure shows a slightly simplified conventional rig set up of the hoisting system. The Load Indicator measurements are used to calculate the weight suspended in the hook (Bourgoyne et al. 1986).

[1] Personal communication with Thor Arne Brandsvoll. 2012. Kristiansand, Norway: Aker Solutions.

The block-and-tackle arrangement in the top of the derrick increases the pulling capacity and reduces the pulling speed. This is favorable since the needed pulling capacity typically is in the range of several hundred tons and the speed is limited upwards to maximum of about 1 m/s due to considerations such as swabbing pressure, well stability and to some degree limitations of the equipment. The relationship between the weight of the travelling block and suspended loads to the tension in the deadline in an ideal and frictionless pulling system is expressed as:

$$W = F_{dl} \cdot n \tag{1}$$

Here W is the travelling block weight and suspended loads in the hook, F_{dl} is the tension force in the deal line, while n is the number of lines strung through the travelling block (string up).

This simple relationship does not account for friction effects or movement direction. Dangerfield (1987) did an analysis on friction resistance in the sheaves to check the accuracy of the current accepted weight indicator models. While pulling the hook upwards and coming out of the hole, he stated that friction effects will be added from the dead line, through the sheaves and to the fast line. This effect makes the tension gradually reduce from the fast line to the dead line when pulling out, and the other way around when lowering into the hole. Luke and Juvkam-Wold (1993) confirmed the effect and concluded that the currently used calculation methods predicted values with errors up to 19 %, and proposed more detailed equations taking into account the movement direction, inactive sheaves and sheave efficiency. The average sheave efficiency in their experiments was 89 %. To compensate for the friction losses and tackle arrangement, they proposed the use of the Inactive Dead-Line Sheave Model given by the equations:

$$W_{hoisting} = F_{dl} \cdot \frac{e \cdot (1 - (1 / e^n)}{(e - 1)} \tag{2}$$

$$W_{lowering} = F_{dl} \cdot \frac{(1 - e^n)}{(e - 1)} \tag{3}$$

Here $W_{hoisting}$ is the predicted hoisting weight, $W_{lowering}$ is the predicted lowering weight and e is the sheave efficiency.

New equipment to be used in the hoisting system includes increased number of high accuracy measurement points[2]. This report will leave the measurement methods, procedures and prediction models at this level and not discuss it further. Hereafter throughout this report, HKL values are assumed to be corrected for method, system friction, direction and other effects that influence the measurements values.

2.3 Drill String Weight

The drill string can roughly be decomposed into two kinds of pipe type; bottom hole assembly (BHA) and drill pipe. The BHA is a collective term used to describe the bit, tools and drill collars at the bottom of the string. The rest of the string is then described as drill pipe. The drill pipes function as a torque and force communicator from the rig to the bottom of the hole, while the BHA supplies the needed weight for cutting and crushing the rock as well as the necessary equipment for direction control, measurements sensors etc.

2.3.1 Gravity

When speaking of the weight of the drill string, it is common to use the term *unit weight*. Unit weight is weight per length and is defined as:

$$w_{air} = \rho \cdot A_{cs} \cdot g \tag{4}$$

Here w_{air} is the unit weight of the drill string element, ρ is the density of the drill string material and A_{cs} is the cross sectional areal of the pipe. Multiplying the unit weight with the length of the element, then gives the weight in air:

$$W_{air} = w_{air} \cdot L_{element} \tag{5}$$

Here W_{air} is the weight of the drill string element in air and $L_{element}$ is the length of the drill string element.

[2] Personal communication with Thor Arne Brandsvoll. 2012. Kristiansand, Norway: Aker Solutions.

Knowing the involved parameters will give the static weight of the drill string and furthermore, a value of the HKL. This is the static weight with the bit off bottom in a vertical wellbore, not considering inclination, restrictions, drilling fluids or any other factor influencing or reducing the weight.

2.3.2 Buoyancy

Having a well filled with fluids makes the drill string feel a lifting force called buoyancy. The buoyant force depends on the densities and volumes of the materials present, and is defined by the Archimedes principle; "an object totally or partially immersed in a fluid is buoyed up by a force equal to the weight of the fluid that is displaced". Defined in oil field language; "The net effect of hydraulic pressure acting in a foreign material immersed in the well fluid is called buoyancy" (Bourgoyne et al. 1986).

The common way of correcting for this uplifting force is to multiply the drill string weight by a buoyancy factor (β). The well is filled with mud and most of the drill string pipes are made of steel, thus the factor will be expressed as:

$$\beta = 1 - \frac{\rho_{mud}}{\rho_{steel}} \tag{6}$$

Steel has a density of 7840 kg/m^3 and drilling fluids (mud) may vary from sea water, having a density of 1025 kg/m^3, to heavy drilling fluids exceeding 2000 kg/m^3. This gives typical values for the β in the range from 0,85 down to 0,75 and will accordingly reduce the measured weight of the DS between 15 to 25 % relative to the weight in air. An important note to the use of a buoyancy factor is that it assumes a drilling fluid with constant density. The two most important tasks for the drilling fluid are to remove the drilled rock parts, cuttings, from underneath the bit and then transport them up to the surface (Skalle 2011). Rock cuttings together with inflow of formation fluids are the dominating parameters that affect the density of the drilling fluid column and could, especially if hole cleaning is inadequate, lead to significant difference in local density. Cutting will however not be present in the mathematical model, and will therefore not be discussed further in this report.

The result of the buoyancy is a net experienced weight of the pipe element expressed as:

$$W = W_{air} \cdot \beta \tag{7}$$

This simple derivation results in Eq. (7); the free hanging weight of a drill string element submerged in fluid. To obtain the weight of the whole string, all the segments (with lengths equal to $L_{element}$) are added together. This equation gives accurate estimations and can be used with confidence if the needed parameters are known.

As the well digs deeper and builds angle, the conditions change. The major contributor to change in experienced weight in the hook in these circumstances, is the contact forces between the drill string and bore hole wall; the friction.

2.4 Friction

Aadnøy and Andersen (2001) stated that well friction is one of the most important parameters limiting the extended reach drilling. Aadnøy et al. (2010) later stated the importance of friction analysis not only during drilling, but also in completion and work over operations.

All kinds of friction have one thing in common; it strives to resist motion. It is like a stubborn old man resisting change. This stubborn old man is defined as ”the force between surfaces in contact that resists their relative tangential motion” (Elert 1988). The relative tangential motion is understood as the sliding behavior between two surfaces of interest and it acts the opposite way of the relative motion. The stubborn old man can be divided into[3];

- Dry friction
  - Between two solid surfaces
  - Static friction and dynamic friction
- Lubricated friction
  - Two solid surfaces separated by a thin fluid layer
- Skin friction
  - Moving a solid material through a fluid
- Fluid friction

[3] Wikipedia. 2012. Friction (10 January 2013 revision), http://en.wikipedia.org/wiki/Friction (accessed 12 January 2013).

- Between layers within a viscous fluid

- Internal friction
  - Related to material stiffness and deformations

The challenge is to accurately estimate these resisting forces. The following subchapters will focus on describing the effects and relevant situations, including dry, lubricated and skin friction, that occur in the borehole and they will use a simple and conservative approach.

2.4.1 Dry Friction

In a well with good hole conditions, dry sliding friction is concluded to be the dominating source of drag (Johancsik et al. 1984). In the same paper, drag is defined to be "the incremental force needed to move the pipe up or down in the hole". Xie et al. (2012) stated that "in a simple model, drag is the increased / decreased apparent hook load when tripping plus the observed rotating hook-load at the equivalent depth". The rotating hook load used by Xie et al. (2012), is during good hole conditions, assumed to be the buoyed weight of the drill string (Cayeux et al. 2012a), where the buoyed weight is the unit weight multiplied by the projected height, independent of inclination angle (Aadnøy et al. 1999). This is due to all frictional forces acting in the rotating direction instead of the axial direction when rotating. To get a feeling of the friction force, the coulomb friction model will be used for explanation. Eq. (8) is a frequently used method to give an approximate value of the force of dry friction. It is the simplest form of coulomb friction.

$$F_f = \mu \cdot F_N \tag{8}$$

Here F_f is the friction force, μ is the friction factor (FF), or coefficient of friction (CoF), and F_N is the normal force. Eq. (8) assumes a linear relationship between the friction force and the normal force. The normal force could be said to be the force caused by an object pushing back on another object which is pushing on it (Fendley 2001). Fig. 2 shows an inclined plane that exerts a normal force on the object due to the weight of the object. The coefficient of friction will be discussed more in detail in sub chapter 2.4.5 Static and Dynamic Conditions, for now it is said to be the stubbornness of the old man (or more academically; how much the surfaces resists the sliding motion).

Fig. 2 illustrates the concept of dry friction and CoF when pulling an object upwards along an inclined plane. This widely used sketch and the concept is the most common way of illustrating friction between a drill string and the borehole wall.

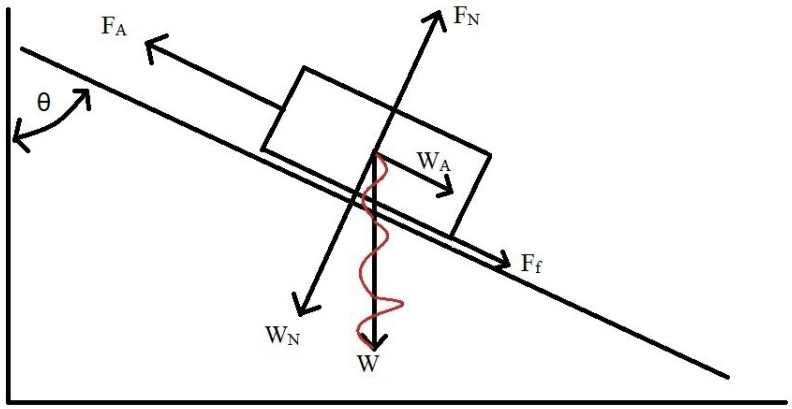

Figure 2: The figure shows the forces acting on an object being pulled along an inclined plane. The weight is decomposed into a normal vector and an axial vector, W_N and W_A respectively.

The force needed to pull the object, F_A , is expressed as:

$$F_A = W \cdot \cos(\theta) + \mu \cdot F_N \tag{9}$$

Here θ is the inclination angle. The gravity force, W , is here decomposed into an axial and a normal component. The first term in Eq. (9) is the gravity component in the axial direction; W_A , while the second term is the friction force, F_f (referring to Eq. (8)), resisting motion in the axial direction. The normal force is strictly speaking as defined in Eq. (9), but is assumed to be $F_f = \mu \cdot W \cdot \sin(\theta)$ if the gravity force is dominating. The normal force can be caused by other phenomena than the gravity force. Other big contributors are the stiffness of the pipe and non smooth hole with a lot of tortuosity.

2.4.2 Side Forces

The dry friction force explained in previous subchapter is exemplified by using the gravity force as normal force. But the normal force can be caused by bending and tension of the drill string as well. Some wells drilled today are still vertical, especially exploration wells with only one target of interest or targets in the same vertical direction, but most wells include vertical and azimuth deviation. This causes side forces to be exerted to the drill string. Fig. 3 illustrates this phenomenon.

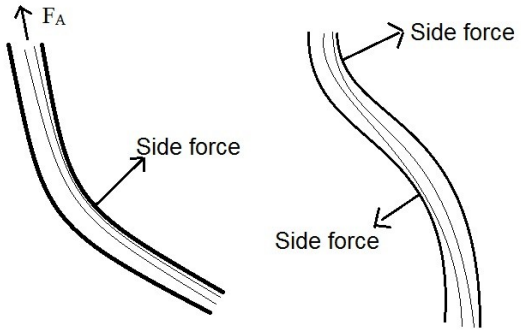

Figure 3: The illustration to the left shows the side force in the "high side" of the well during tripping out. The illustration to the right shows side forces due to the bending stiffness of the pipe caused by a big change in well path (dog leg).

The drill string experiences both compression and tension forces depending on the operation mode and position in the string. In a tripping situation the drill string is, under good well conditions, solely stretched and the tension force results in additional normal forces.

2.4.3 Lubricated Friction

Lubrication is defined by NASA (1971) as “the process by which any foreign substance is interposed between contacting surfaces undergoing relative motion.” The foreign substance may include dirt, oil, grease, chemical coatings, sand, oxide films (including rust) etc.

The lubricating effect tends to reduce the experienced friction force indicating a reduced friction factor (Xie et al. 2012). Relating to the friction between the drill string and the borehole wall, the drilling fluid and particles present in the well would act as a lubricating substance. Maidla and Wojtanowicz (1990) conducted experiments showing

that the friction coefficients are affected by mud quality, mudcake and lubricant additives. By example, the presence of mudcake caused an initial reduction of the average friction coefficient from 0.23 to 0.17. The paper summarizes a collection of tests and the authors showed a significant difference between water based mud (WBM) and oil based mud (OBM). The OBM adds a higher lubricating effect than water based ones. Through laboratory experiments, Skalle et al. (1999) found that small polymer micro beads added to the drilling fluid could reduce the friction factor in water based muds with as much as 40 %.

It is often difficult to predict the magnitude of these lubricating effects. The difference from experimental calculated friction reduction to the experienced effect when applied in the field is often significant (Maidla and Wojtanowicz 1990).

2.4.4 Skin Friction and Hydraulic Viscous Forces

The skin friction, or hydraulic drag, is the friction effect that fluids exert when pulling a solid object through it. Assuming that the drill string is static at rest in the hole and the hook starts pulling upwards, the drill string will then start tripping out of the hole. Since the drilling fluids have high viscosity, it will stick to the drill string and try to hinder it from moving. In addition, the hoisting of the drill string will create a removed volume at the end of the drill string, resulting in an effect known as swab. This removed drill string volume is illustrated by the white dotted box in Fig. 4. The drill string is colored green, the two lines on each side illustrating the borehole walls and the curved line to the left shows the velocity profile of the drilling fluid. The removed volume reduces the local pressure and hence results in a net force downwards acting on the drill string end area.

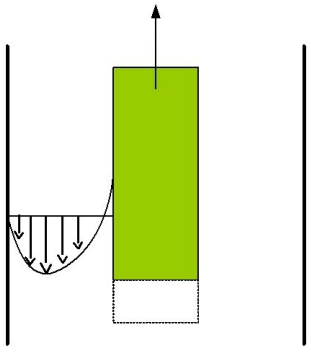

Figure 4: The drill string (green) is pulled upwards and creates a void space (white dotted box). The removed volume causes a lower local pressure which again results in a suction of both the drill string and fluids towards the lower pressure zone (free after Skalle 2011).

These to phenomena will increase the force needed to trip the drill string out of the hole. A simple derivation (Mme et al. 2012) estimates the skin friction force;

$$F_{skin} = \frac{\pi \cdot OD_{pipe} \cdot \tau \cdot L}{HS - OD_{pipe}} \tag{10}$$

Here τ is the shear stress at the surface of the pipe and the other parameters are found in the abbreviations list. The skin force is highly dependent on the annulus clearance ($HS - OD_{pipe}$). This makes the smaller hole sections, e.g. the 8 ½" sections, specifically sensitive to this effect due to the low annulus clearance (Mason and Chen 2007).

If the hole is circulated during tripping, and the fluid volume pumped in exceeds the removed drill string volume, the forces will act the opposite way since fluid will flow up through the annulus. The skin friction and the force acting on the end of the drill string, is highly dependent on the flow rate and the pressure loss in the annulus. Mason and Chen (2007) stated that some models include this effect, but several models ignore it.

2.4.5 Static and Dynamic Conditions

The simple form of the coulomb friction presented in Eq. (8) needs some words of explanation. Assuming an object resting on a horizontal surface with a known empirical CoF and known weight, being applied a pulling force. The pulling force is applied, but the force is not enough to make the object move: the friction acts against. It is only the gravity force acting downwards, resulting in a normal force acting upwards, and the pulling and friction forces, which are acting in opposite directions (ref. to Fig. 2), that are present. The friction force increase exactly as much as the pulling force until the object suddenly starts moving; the friction has been overcome. Assuming a constant pulling force, the friction force is reduced after the object started moving. The weight of the object, and thus the normal force, is certainly not reduced. To mathematically take this effect into account in the coulomb friction model, the static and dynamic CoF are introduced, μ_s and μ_k respectively.

The CoF presented earlier in this chapter does not take into account the change when moving from static and dynamic conditions. The coefficient of friction, or the stubbornness of the old man, is an empirical value that is limited to the contact behavior between two dry, cleaned and specified materials. The value is determined by measuring the magnitude of the friction force relative to the known normal force, illustrated by Eq. (11):

$$\mu = \frac{F_f}{F_N} \tag{11}$$

By gathering CoF values experimentally and knowing the materials and surfaces involved, a predicted frictional force can be calculated. A measurement signature plot of the frictional force from a static to a kinetic (dynamic) movement is shown in Fig. 5. A constant increase of pulling force is here applied until the object starts moving. The force needed to keep the object in motion is less than the one that was needed to make it start moving.

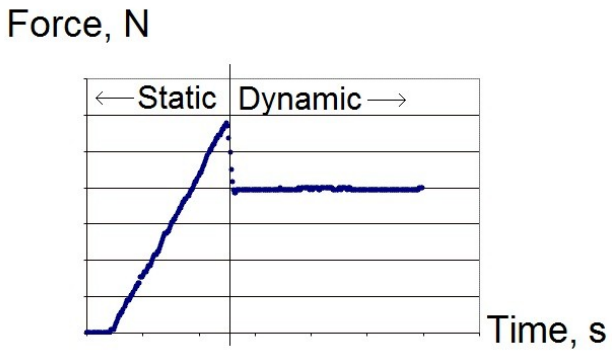

Figure 5: Change in friction force when going from static to kinetic friction. An increased pulling force is applied until the object starts moving, thereafter a constant pulling force is applied and the difference in static and kinetic CoF is illustrated (Hart 2013).

This implies that the static friction usually is larger than the kinetic friction and thus obeys the inequality;

$$\mu_k < \mu_s \tag{12}$$

Table 1 shows example values of static CoF, μ_s, for some well-known material combinations. As the table shows, the static CoF can even be greater than 1 for some material combinations.

Table 1: CoF for some selected pair of materials[4].

Material Combinations		Static CoF, μ_s	
		Dry and Cleaned Surfaces	Lubricated and Greasy Surfaces
Aluminum	Steel	0.61	
Aluminum	Aluminum	1.05 – 1.35	0.3
Concrete	Wood	0.62	
Steel	Steel	0.80	0.16
Steel	Teflon	0.04	
Iron	Iron	1.0	0.15 – 0.20
Graphite	Steel	0.1	0.1

In drag modeling, the FF is the most significant unknown parameter (McCormick and Liu 2012). A FF should ideally solely represent the described relationship between the mechanical normal and friction force. Due to the complex conditions and behavior in the hole, other effects, that the model does not account for, are included in the FF to make it fit the measured values. This is the reason why the term "fudge" is sometimes used to describe the FF. Due to this, such a model would often underestimate the friction forces or compensate by overestimating the friction factor (Ho 1988). Some main unwanted contributors to increased FF estimation (Mason and Chen 2007) are;

- Pipe stiffness effects (not included in soft string model)
- Viscous drag (fluid resistance to pipe movement and fluid circulation)
- Cuttings bed (mechanical wellbore obstructions)
- Formation types (variation in lubricity)

[4] Engineering ToolBox, 2012. http://www.engineeringtoolbox.com/friction-coefficients-d_778.html (accessed 5 November 2012).

Talking about lubricity, the presented material in the subchapter of lubricated friction indicated that the friction factor could be reduced by over 20 % in the presence of a mudcake (Maidla and Wojtanowicz 1990). It would be difficult to include the mudcake effect in a mathematical model, even harder to decide whether it is present or not (!). Xie et al. (2012) stated that conventional FFs include these kinds of effects when they are not implemented in the model. This is supported by Mirhaj et al. (2011).

FF during drilling may vary depending on the well conditions as mentioned. Johancsik et al. (1984) reported FF from 0.25 to 0.40 in partially cased hole with WBM. Sheppard et al. (1987) reported values around 0.36 for WBM. Mason and Chen (2007) stated that for the majority of rotary drilling operations, the dynamic CoF ranges from 0.10 to 0.30 having extreme values as low as 0.05 and high side of 0.50.

2.5 Inertia forces and Elastic Behavior

Eq. (13) expresses Newton's second law: "Applied force is the product of mass and acceleration".

$$F = m \cdot \frac{dv}{dt} = m \cdot a \tag{13}$$

Inertia is the object's resistance to change its direction of motion. Inertia and mass are like the cousin of friction, the stubborn old man; the more the mass, and thus inertia, the more the object will resist acceleration. The direction of motion of the drill string will constantly change and thus accelerate.

When an object is subjected to a tension or compression force, the object might deform. The relationship of how much the object deforms when subjected to a force is described by different moduli. The modulus is a material property and varies much between materials. To describe elastic behavior of a material when subjected to a tension force, the Young's modulus is often used. Elastic behavior is used when the material returns to its original shape when the force is removed. Elastic deformation does not lead to any permanent deformation of the object. Eq. (14), (15) and (16) defines the parameters.

$$\sigma = \frac{F}{A_{cs}} \tag{14}$$

$$\varepsilon = \frac{\Delta L}{L} \tag{15}$$

$$E = \frac{\sigma}{\varepsilon} \tag{16}$$

Here σ is stress, F is applied force, A_{cs} is cross section area, ε is strain, L is initial length and E is Young's modulus. The moduli are values assigned based on the slope of the curve in a stress versus strain plot of experimental obtained measurements. Such a plot is shown in Fig. 6.

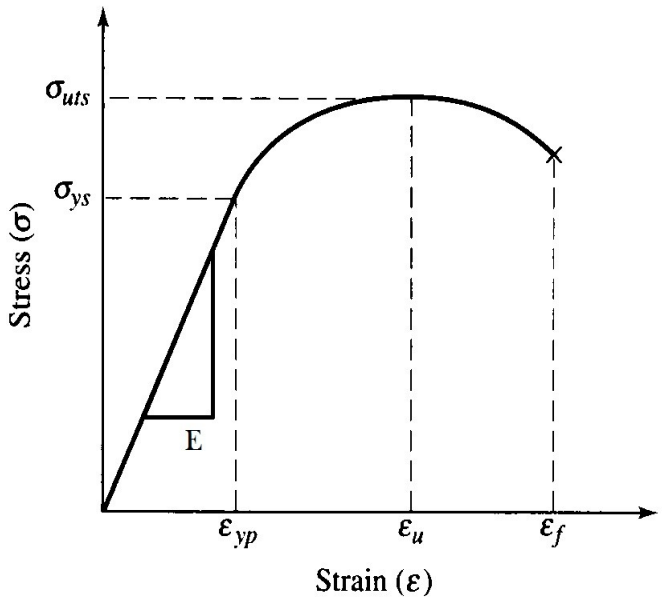

Figure 6: Stress versus strain curve for elastic materials. The materials follow a curve during any tensional load, starting at origin. If the stress applied is less than the yield stress (subscript ys), the material will return to its original shape after removing the applied force. If the yield stress is surpassed, permanent deformation will occur (Best 1990).

To illustrate the effect of this elastic behavior, a simple calculation will be done. Putting Eq. (14) and (15) into (16) results in:

$$E = \frac{F / A_{cs}}{\Delta L / L} \tag{17}$$

Solving for ΔL gives:

$$\Delta L = \frac{F \cdot L}{E \cdot A_{cs}} \tag{18}$$

Assuming that the drill string is stuck at the bottom of the hole and the driller experiences 25 tons overpull (incidence in Fig. 17), having a drill string of 1563 mMD composed of steel drill pipes of OD of 5" and ID of 4,276", the string stretches:

$$\Delta L = \frac{25 \cdot 10^3 kg \cdot 9,81 \, {}^{m}\!/_{s^2} \cdot 1563m}{210 \cdot 10^9 \cdot {}^{N}\!/_{m^2} \, \frac{\pi}{4} \cdot (5"^2 - 4,276"^2) \cdot \left(\frac{0,0254m}{"} \right)^2} = 0,53m \tag{19}$$

This behavior of the elastic drill pipes might influence the signature plot of the field measurements of the HKL. This is the behavior that is tried modeled with the mathematical spring model and will be discussed later on.

3 Previous Work

Many approaches in trying to model the suspended weight in the hook have used a trend basis while pulling stand by stand of drill pipe out of the hole. Examples of "per stand" time span are the ongoing thesis work by Bjerke (2013), based on the work by Cordoso et al. (1995); interpreting signal plots in order to identify and diagnose troublesome behavior, and the complex integrated software developed at IRIS in Stavanger. By looking at a limited time interval, potential trouble can be recognized at an earlier stage.

A model developed at the department of petroleum engineering and applied geophysics at NTNU (Mme et al. 2012), estimates the HKL by assuming that the force needed to pull the drill string out of the hole can be modeled by including the calculated weight, the friction force as a function of normal force caused by weight, fluidic drag and the elastic behavior modeled by a mass-spring system. The parameters in the model are calculated separately (and kept static,) having no dependency on things like temperature, inhomogeneous drilling fluid (e.g. by cuttings), variations in friction factor (from open hole to cased hole), points of contact between the drill string and the borehole wall, erosion of the drill pipes, side forces etc.

According to Cayeux[5], an optimal model would include for the mentioned things and should have them interconnected. New information from the RTDD should automatically be put into a complete well model and continuously update all the other parameters. In addition, equipment such as float subs etc. should also be accounted for in an optimal model. To include for the points of contact between the drill string and the hole wall, Timoshenko's beam theory could be applied[5]. Successful attempts of such global models have been done at IRIS in Stavanger and are documented by several papers (Cayeux et al. 2012a, 2012b; Cayeux and Daireaux 2009.).

In a trustworthy model, the sample frequency of which the parameters are recorded should be of a sufficient rate to be able to "catch" the elastic behavior due to the acceleration of the drill string and other effects appearing in a short time interval[6]. Cordoso et al. (1995) concluded that a sampling rate of less than 3 Hz is inadequate to record the acceleration effects of the string.

[5] Personal communication with E. Cayeux (Chief Scientist). 2012. Stavanger: IRIS (International Research Institute of Stavanger).
[6] Personal communication with T. Toverud. 2013. Trondheim: External consultat at NTNU.

The next sub-chapters are based on material and work done in relation to the project thesis (Kristensen 2013), written by the author of this report. The chapter will present the main history and development of friction prediction models as a literature study to better understand the phenomena and check the status of present models. Due to the extensive comparison of existing and slightly improved models to previous models and field data, this report limits itself to present the soft and stiff string models. The soft string model will be presented with mathematical equations.

3.1 Mathematical Models

The aim of a model of drilling parameters is to as accurate as necessary predict how the parameters are expected to develop during the planned operation. If the quality of the model is good, it is calibrated and simulates the conditions sufficiently, any deviation from it could be interpreted as abnormal well behavior. This will give useful information and will indicate what remedies are needed to improve well conditions. To know the ideal and normal behavior is thus of high importance. The overall challenge is to know what is really going on in the hole and implement it all into a model; basically knowing what normal conditions are. The cased hole conditions exclude a great deal of potential trouble. In normal circumstances the cased hole will keep a constant and known hole size and will not react with the formation. In addition, it is easier to estimate and assign a FF to this part of the hole as the present materials are known. The open hole introduces a number of other effects and is thus harder to predict. Well known open hole problems are wash outs, tight hole conditions, key seats and cuttings build up due to poor hole cleaning. These situations all give abnormal drag responses (Johancsik et al. 1984).

In addition to analytical and mathematical calculations of the friction and drag estimations, trend analysis will be presented and explained. The latter method is used to detect *changes* in downhole conditions, without the need of a highly accurate model. By making plots of the measured values over a period of time, the trend of how the conditions are developing, can be registered and thus predicted further ahead.

The concepts presented in the previous chapter are examples of how the friction phenomena can be applied to a friction model. The model presented by Johancsik et al. (1984), often referred to as the “soft string”, “chain” or “cable” model, was the start of systematic friction modeling. This method was improved and later on presented in a

differential form by Sheppard et al. (1987), who also included the fluid effects and gave a suggested well path to minimize friction. Due to its simplicity and sufficient accuracy, the model has been extensively used in the industry (Mirhaj et al. 2011). The need for a higher prediction quality of well friction, especially with respect to the high friction in extended reach drilling, has introduced other modeling concepts. A "stiff string model" concept was early on proposed as an extension of the soft string model. A stiff string model takes into account the bending stiffness effects of the string in the hole. According to Mason and Chen (2007) a number of different techniques have been used to simulate this behavior.

3.1.1 Soft String Model

The soft string model introduced by Johancsik et al. (1984) assumes that drag is caused solely by sliding friction forces resulting from the contact between the drill string and the wellbore, illustrated by Fig. 7. Other sources of friction are not considered in the model.

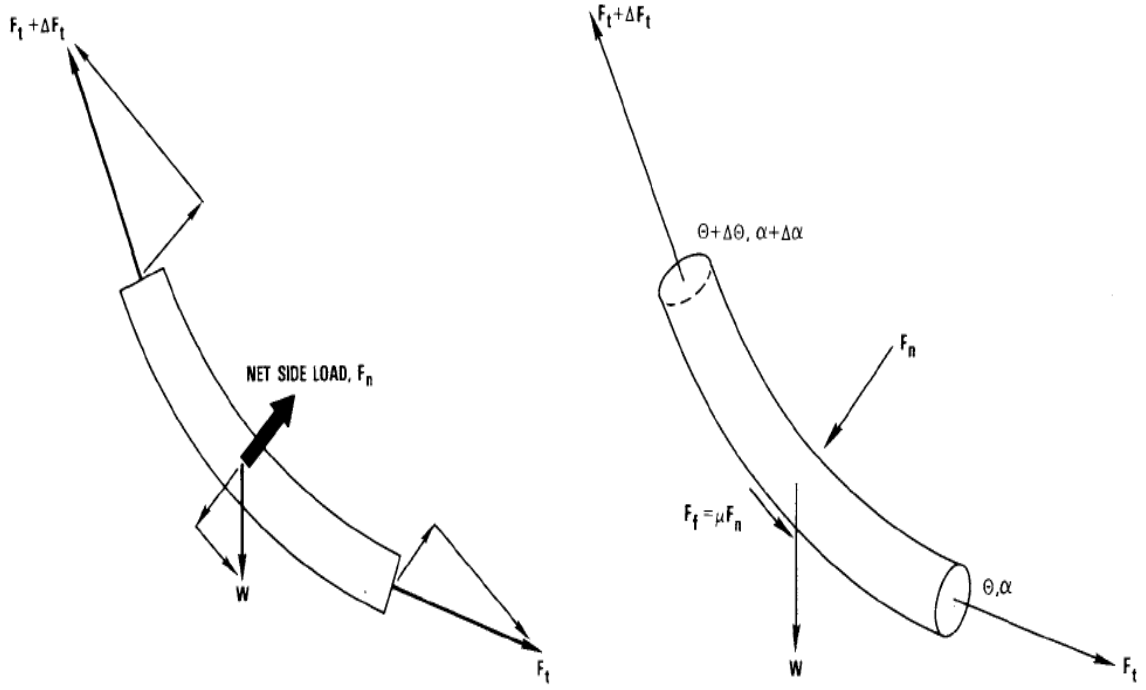

Figure 7: Forces acting on a drill string element, illustrating the normal force, friction and changes in inclination and azimuth. This figure is the original one, posted by Johancsik et al. (1984).

In Fig. 7, θ and α represents inclination and azimuth respectively, and F_t is the tension in the drill string. These parameters are used to calculate the additional normal forces due to tension in the drill string. In the model they assumed the standard Coulomb friction method and set up a force balance for a drill string element (as exemplified in chapter 2.4.1). The normal force is here assumed to be entirely caused by the gravity component of the element and the tension of the element against the wellbore wall (, and thus excluding the bending stiffness). By dividing the drill string into these elements, the calculation method is performed on each one from the bottom and up to the rig. Starting the calculation from the bottom of the string ($n = 1$), using the counter n and $n+1$, instead of t and $t + \Delta t$. Assuming a straight hole section, the equation yields:

$$F_{n+1} = F_n + w_{unit} \cdot L_{element} \cdot [\cos(\theta) + \mu \cdot \sin(\theta)] \tag{20}$$

By introducing curvature of the hole like in Fig. 7 the normal force changes and the equation yields:

$$F_{n+1} = F_n + w_{unit} \cdot L_{element} \cdot \cos(\bar{\theta}) + \mu \cdot F_N \tag{21}$$

Here;

$$F_N = \sqrt{[F_n \cdot \Delta\alpha \cdot \sin(\bar{\theta})]^2 + [W \cdot \sin(\bar{\theta}) + F_n \cdot \Delta\theta]^2} \tag{22}$$

$$\bar{\theta} = \frac{\theta_{n+1} + \theta_n}{2} \tag{23}$$

$$\Delta\theta = \theta_2 - \theta_1 \tag{24}$$

Equations (23) and (24) applies for the azimuth changes, α, as well. Sheppard et al. (1987) had a theory that the well trajectory had an influence on the total experienced torque and drag. They put the soft string model proposed by Johancsik et al. (1984) into differential form and included mud pressure forces, in the form of shear and pressure, in the model to obtain an “effective tension”. For more detailed development of the model, the chronological history of the numerous improvements of the soft string model is given by Mirhaj et al. (2010) and includes the large number of changes made by Aadnøy et al. (1999; 2001; 2010).

3.1.2 Stiff String Model

Ho (1988) tested the model proposed by Johancsik et al. (1984). He pointed out the weaknesses of a model completely based on a soft string concept, and introduced their stiff string ideas to be applied to the stiffer parts of the drill string, mainly the BHA. Ho found that the soft string model performed well in smooth well trajectories and that the stiffness is negligible for the part of the drill string consisting of low stiffness drill pipe, but needed another model to predict the stiffer part. This was one of the first attempts of taking the stiffness into consideration. Including pipe stiffness, wellbore radial clearance, dog leg severity and tortuous well trajectory, a more realistic model should be achieved (Mason and Chen 2007). It does not exist an industry standard formulation of this model type (Mitchell and Samuel 2007), so when referring to "the stiff string model", it includes all the methods and models aiming to include the mentioned effect. The effects that the stiff string model aims to implement increase in relevance today as the trajectory and length of wells increase and wellbore radial clearance reduces. To include the mentioned physical effects, significant more comprehensive mathematical models are used. These include finite difference (Ho 1988), finite element (Andrew et al. 2011) and semi-analytic methods. To make a stiff string model perform optimal, there is a need for sufficient resolution and availability of survey and equipment data (Mason and Chen 2007).

3.1.3 Discussion About Model Development

The need for more accurate and comprehensive models followed the drilling of longer and more complex wells during the 1990's (Mirhaj et al. 2010). An analysis done by Mason and Chen (2007) stated that the current collection of available T&D software had not changed significantly since the program made by Johancsik et al. (1984). As pointed out earlier, the model has been improved numerous times, but the foundation is still the same. The paper by Mason and Chen (2007) declares that the time has come to reflect upon the current models and identify future model requirements. This statement is supported by Mirhaj et. al. (2011) which says that friction models today do not take into account all the effects that are present in the well. They point out the importance of including tripping speed, hydraulic effects, stiffness and piston effect of packed stabilizers in the BHA.

3.1.4 Real Time Model Update and Trend Analysis

Vos and Rieber (2000) used a so called "real-time torque and drag technique" on a field development by using current drilling conditions automatically and directly in the model calculations. In this way, the models where automatically calibrated with updated input. An illustration of the model inputs is shown in Fig. 8.

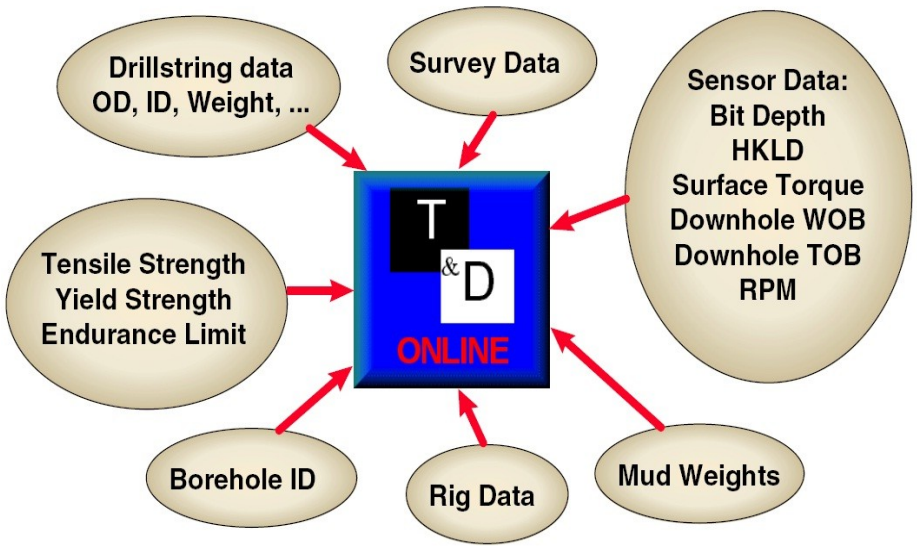

Figure 8: Illustration of the input parameters to the automatically updated models where RTDD was used in a field development offshore Denmark (Vos and Rieber 2000).

The obvious benefit of using real time data as input to any model, compared to off-line and pre-calculated ones like Falconer et al. (1989), is that more correct values are used and thus giving more accurate results. These parameters are among others correct mud weight, actual well path etc.

Niedermayr et al. (2010) presented the method of Falconer et al. (1989) in an automated form, as Vos and Rieber (2000) did, and focused on trend analysis to detect abnormal hole conditions. The chart showed in Fig. 9 serves as an example output of a hook load chart. In the figure, the modeled and estimated normal hook load is drawn as the continuous blue and red lines and measured vales are plotted in the chart.

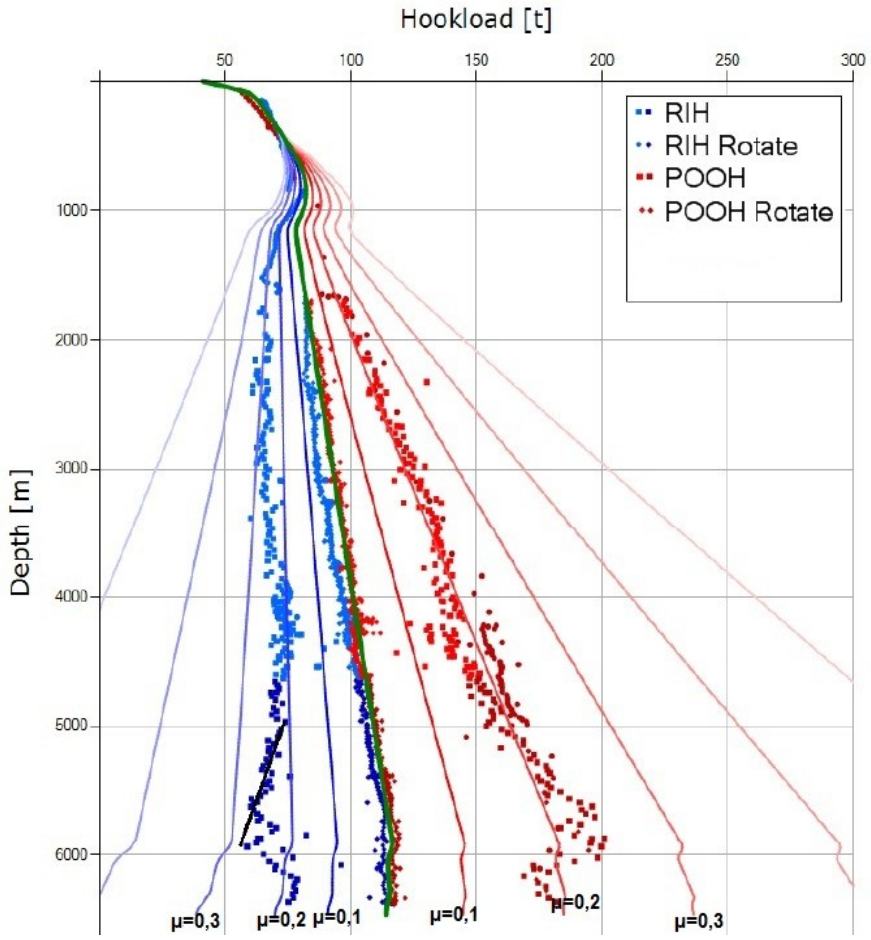

Figure 9: An example output from a T&D model. The solid lines are outputs with different CoF and the squares and dots are measured values (see nomenclature for operational description). It can be seen that the excessive loads, compared to the estimated and modeled values, were experienced from 5000 m while running in hole (blue dots and squares to the left). This is observed as an increase in friction factor and illustrated by a black line. The hole conditions start to return to normal after 6000 m (modified from Niedermayr et al. 2010).

Not only is the complexity of the physics is difficult to model, also the *history* of the well plays an important role and has to be taken into account if an accurate and high quality model is needed. The well is affected by all the operational activity it is being exposed to; drilling, tripping, circulation, temperature changes, stop in circulation, high circulation etc. The work done by Cayeux et al. and International Research Institute of Stavanger (IRIS) in the development of the software DrillTronics and DrillScene aims to implements all such effects in a total package. This includes not only software programs but also some hardware modifications to be able to record the needed

measurements. This method is summarized in Cayeux et al. (2012b) by several case studies and further exemplified in Cayeux et al. (2012a). The case studies have proven to manage to predict hole problems long before the drilling rig and operational team. In addition, the case studies managed to assign the correct diagnosis, when the operational team executed wrong remedies. An example of such a situation is presented in chapter 3.4 Practical Application of Model Output (Fig. 10).

This way of modeling the well is different from treating the physical elements separated. They all influence each other. Most service companies now offer such a comprehensive software modeling package to their clients[7].

3.2 Modeling Software

The value of a good torque and drag model in all phases of a well operation is not doubted in the industry. It started with Johancsik et al.'s (1984) computer program that was developed together with the proposed soft string model. The program was tested against 3 well sections and concluded realistic predictions. This was the start for systematic T&D software modeling.

The value of giving a good prediction of the magnitude and direction of the forces expected in a drilling operation in a specified well path is of critical importance. The software predicts and estimates the forces which afterwards are the criteria for the equipment specifications needed to drill the well. It also specifies the limits of a well path to be drilled with given operational equipment.

When the drilling starts, the modeling software monitors the progress of the parameters. Comparing them to the upfront estimated values or to automatically calibrated modes will give indications about the model validity and borehole conditions.

After almost 30 years, it exist a large number of available software to model the forces in the drill string and bore hole. Most of the mathematical equations still have the same foundation and have more or less the same base. Due to the complexity of the conditions in the borehole, models fail to manage all kind of operational modes and the validity of each specific software are heavily discussed (Mason and Chen 2007). Xie et al. (2012) discusses the use of frictional software in complex well operations and presents a model that was used with success on a field case study.

[7] Personal communication with Pål Skalle, Associated Professor, NTNU, 2012.

3.3 Measurement Gathering

The charts and outputs from a friction model are often called roadmaps, illustrated by Fig. 9 and Fig. 10. How the data is gathered, depends on several things. Some models and practices perform manual measurements procedures, interrupting the drilling operation and using valuable rig time. The following procedure is used by Statoil when drilling challenging sections:

1. Collect T&D data in a consistent manner for hole cleaning monitoring.
2. Free string weight to be used for calibration of the simulation.
3. Follow connection procedures.
4. With one single off bottom, shut of pumps and measure off-bottom torque and free string weight (for motors, keep some flow, approx 200 – 300 LPM).
5. Record rotating off-bottom torque and string weight at a consistent RPM.
6. Stop the rotating and pick up at 10 m /min, record pick-up weight (zero or minimum circulation).
7. Shut down the pumps (if not already done) and make connection.

This procedure can be simplified for every stand or performed less frequently (Best Practice Drilling Operations Statoil 2008).

The benefit of doing this operational procedure is an increased focus on the measurements and collection of information. The measurements are calibrated to the parameters during the drilling activity and thus the difference can be seen. On the other hand, the procedure uses rig time and only single values of measurements are obtained. Cayeux et al. (2012a) demonstrated an early warning system which continuously compares the surface and downhole measurements to continuously calibrated and updated physical models. The system analyses, among others, the sliding friction and free rotating weight deviations during the drilling operation. This method both saves valuable rig time and gives a large number of measurement points. The automatically calibrating of the models results in a higher accuracy of the models and better estimation of the hole conditions.

3.4 Practical Application of Model Output

In addition to the drill crew, several people supervise the well conditions; the mud logger, on-shore support personnel and the MWD/LWD responsible person. The driller controls the core of the drilling operation. With respect to detecting deteriorating well conditions during tripping, the main parameters which the driller supervises are the hook load, in the form of overpull, and displacement volume. In this sense, the driller is an important person to detect any changes in the hook load during the tripping activity. With respect to the overpull limit, the driller has a maximum overpull which can be reached before other actions have to be taken[8]. The overpull force is the hook load force used to pull the drill string minus the theoretically estimated needed force, showed in Eq. (25):

$$F_{overpull} = W_{measured} + W_{estimated} \tag{25}$$

The additional force, overpull, is assumed to be caused by restrictions in the hole, but the accuracy of the overpull value is highly dependent on the estimated weight. Due to the dependency on modeled values, the term "overpull" has by some operational teams been tried rephrased by "do not exceed 10 tons above the predicted HKL value on the 0,2 friction factor line at given depth" (Niedermayr et al. 2010). Even though this is a more correct way of saying it, the overpull term still is widely used[8]. The driller also keeps track of the history and development of the hook load, but in complex drilling scenarios there are many parameters to keep track of and this could sometimes be difficult[8].

By monitoring the development of the drilling parameters over a period of time and looking at several parameters at the same time, the highest benefit is achieved. In a complex situation it is difficult to monitor the complete picture of the situation at all times and by predefining the limits and combination of parameters that defines a specific troublesome situations, the software help diagnose the well condition by means of the symptoms. A situation in the North Sea is here used (Fig. 10) to show the benefit of such a tracking and diagnostic software.

[8] Personal communication with Ronny Isaachsen, Driller, 2012. Ocean Rig.

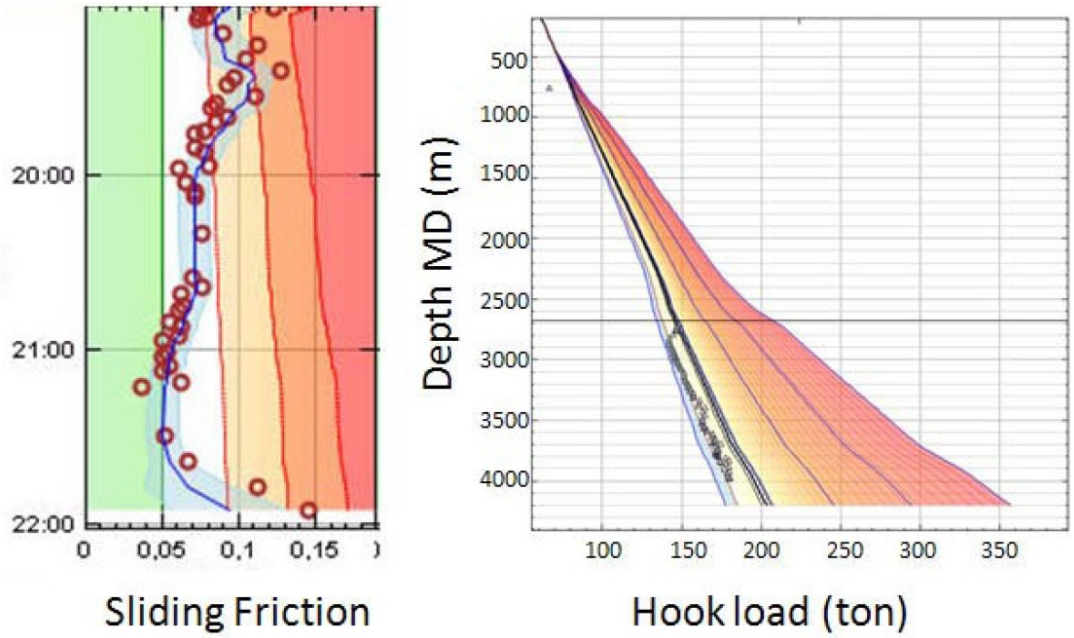

Figure 10: Development of abnormal well conditions during tripping out of a 12 ¼" hole in the North Sea detected by software program before the operational team noticed any trouble. The deteroriating conditions can be seen as a rapid increase in Sliding Friction (factor) to the left in the picture and also the HKL plot to the right reveals this (between 3000 m and 2500 m) (Cayeux et al. 2012a).

The situation illustrated in Fig. 10 was overlooked by the operational crew and 30 minutes after the first alarm was sent by the software, problems were identified by the operational team, as observed overpull. The offshore team interpreted the symptoms to be a ledge while the software pointed out pulling the BHA into a cuttings bed to be the problem, due to the period of constantly increasing friction factor. The remedies initiated to deal with the assumed ledge did not work. First after treating the trouble as a cuttings bed, better conditions were observed. This serves as a good and recent example of how accurate modeling and high quality software can help avoiding trouble and thus NPT.

4 Field Measurements

This chapter is based on material and work done in relation to the project thesis (Kristensen 2013), written by the author of this report. The value of measuring physical parameters during the drilling operation was recognized already in the beginning of the drilling after oil and gas. Florence and Iversen (2010) gave a historical walk through of the gathering of data and the use of sensors in the drilling process. By measuring parameters the drilling crew could keep better track of the drilling process and progress. In the early days, measurements were only displayed live and not recorded for further processing. After some time, recording became industry standard and it was possible to do trend analysis; evaluate how the parameters had changed over time and compare them to similar wells or operations. Even though increase in measurements supply useful and important information, Rae et al. (2005) stated that the culture in the oil and gas industry is to make a lot of measurements and end up not using them. There is no doubt that there is a large amount of data available and lot of troublesome drilling to be avoided if the information could be processes and interpreted in a more effective way.

The HKL parameter was one of the first to be measured (Florence and Iversen 2010). To optimize the drilling progress, maintain good well conditions and prevent the failure of the drill bit and downhole equipment, it is important to know how much the drill bit is pushing against the rock, and hence how much the rock pushes back. When the bit tags the bottom of the well, any further lowering of the drill string will result in weight on bit (WOB). The reduction in measured HKL is equivalent to the applied WOB. The WOB is a much used parameter in the drilling industry and many bit manufacturers state a value of the WOB to be an upper limitation of the force to be applied on the bit.

The field measurements mainly serve as status of the current well status but also as updated input to the model simulations. Fig. 11 shows typical field measurements and the development of increased hook load. While tripping out of the hole and not changing any of the other parameters significantly, the HKL values are expected to decrease due to less drill string in the hole and thus a lower weight suspended in the hook.

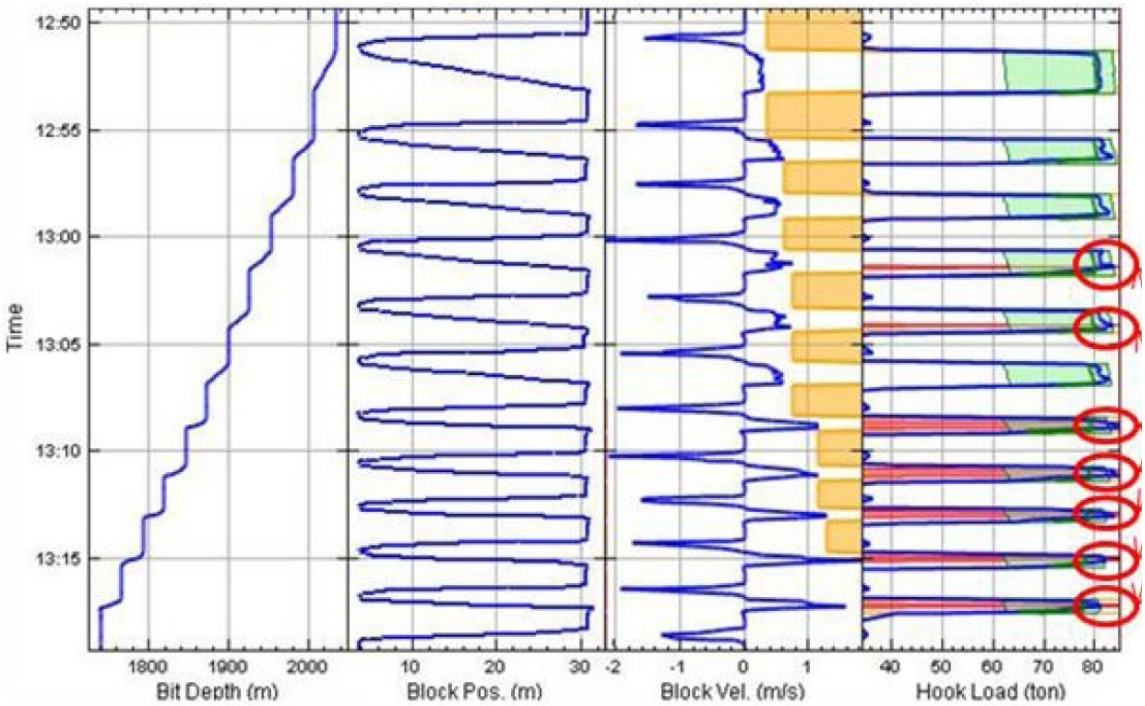

Figure 11: This figure shows how field measurements could be graphically visualized. This example shows how the HKL develops during tripping out of hole. The semi-transient regions in green show acceptable intervals for the HKL, while the red transient indicates too high friction in the hole and suggests remedies to be initiated (also indicated by red rings). The orange regions show maximum tripping speed to avoid high swabbing pressures. In this case the operational crew trusted the modeling software and managed to regain good hole conditions (free after Cayeux et al. 2012a).

4.1 Real Time Drilling Data

The term RTDD basically refers to the situation where drilling parameters are available live during the drilling activity. As described earlier in this report, the most important drilling parameters have been available live during the operation for a long time. The new thing is that this information now, in most cases, is available online through the internet at (onshore) office locations. A big challenge has been, and still is (McLaren et al. 2007), to make a software and hardware interface which automatically detects the changes in downhole environment. The paper by McLaren et al. (2007) stated that the method of trending, up till now (2007), had been limited to the method of visualization. The focus on automated drilling (Florence and Iversen 2010; Cayeux et. al. 2012a, 2012b; Kucs et. al. 2008; Nybø 2009) has showed promising results with respect to reduced time consumption and NPT. But despite promising results and many

case studies, the biggest challenge is to convince the operational team to trust the warning signs prompted by the system (ref. Fig. 11).

4.2 Tripping One Stand

The figures and illustration so far in this report have shown HKL values over an interval of time and the development of the parameter over several connections and stands. Now, the focus will be on the tripping of one single stand (approximately 30 m). To achieve this, the author will investigate RTDD from Statoil to look for field behavior. Fig. 12 shows the equipment used in a tripping procedure.

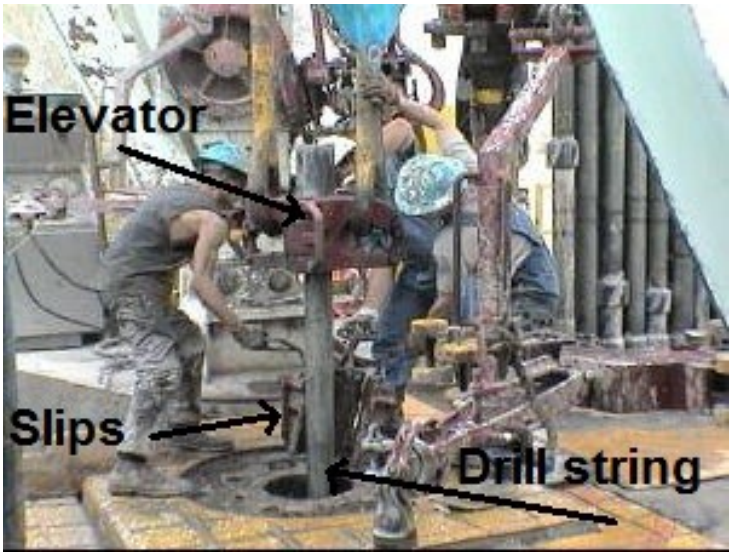

Figure 12: Drill floor illustrating the elevator, drill string and slips. This configuration is consistent with the one presented in Fig. 1 and the two can be combined to get the whole picture. A note to be made is that this configuration is conventional in the sense that a Kelly is used here instead of a top drive (which is more common these days). The weight of the drill string is transferred from the elevator to the hook (not shown in this picture) (Occupational Safety & Health Administration (OSHA) 2010).

Fig. 13 is a good example of how the signature graphs of HKL and block position (BPOS) behaves during this activity. The graphs serve as examples of typical signature plots of a tripping sequence. Starting at the left hand side, the drill string is in slips and hanging freely (off bottom) in the hole. The travelling block (BPOS) goes down to pick up the drill string to trip out of hole. The blue vertical line illustrates the

start of the pulling activity (seen as a small increase in BPOS). The elevator grabs hold of the shoulders of the tool joint and the hook starts pulling the drill string.

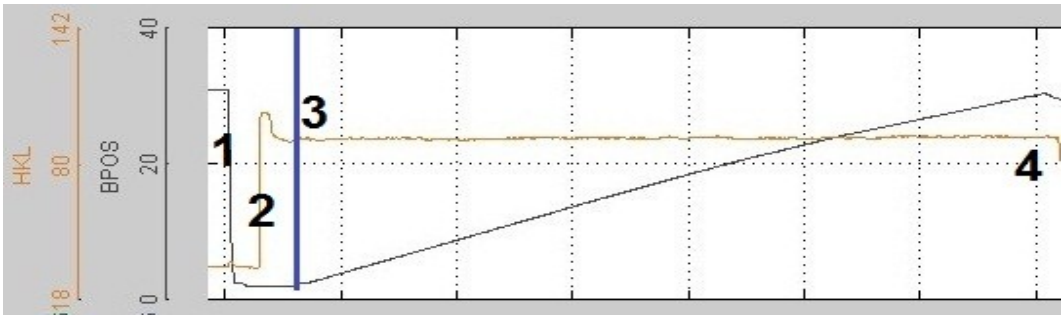

Figure 13: A 17 ½" section at 2034 mMD with a low tripping speed of 0,008m /s (65 min/stand) and circulation of 200 LPM (HKL in tons and BPOS in meters). 1: Hook goes down to pick up drill string. 2: The drill string is connected to the hook. 3 and blue line: Pulling of the drill string starts. 4: Finished pulling drill string and slips are set (RTDD supplied by Statoil).

4.2.1 Good Hole Conditions

Fig. 13 illustrates the behavior during good conditions; the graphs are straight and smooth. To get a more detailed picture of the situation, tripping with a longer string and higher speed is shown in Fig. 14. The smooth behavior of both the HKL and BPOS is maintained.

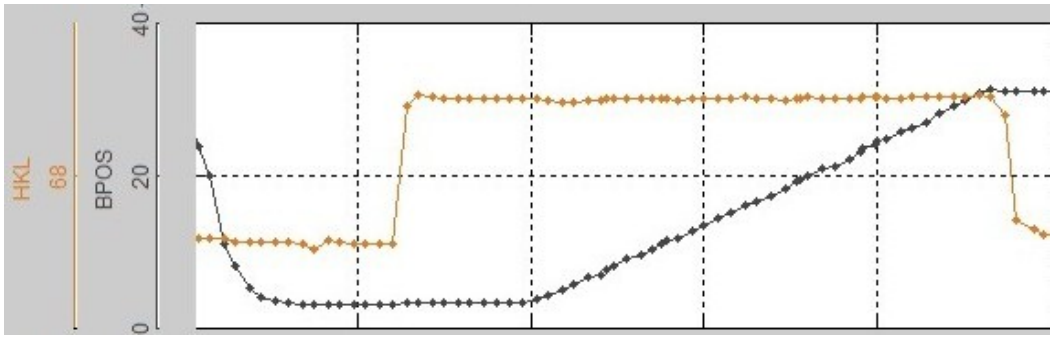

Figure 14: A 8 ½" hole at 3750 m tripped out with a speed of 0,2 m/s (2,5 min/stand) and some circulation. Note the small reduction after the string is accelerated. No first high peak is seen here. This is to further discusses in relation to the mass – spring model (RTDD supplied by Statoil).

The definition of ideal and normal conditions may be difficult to address. Cordoso et al. (1995) state that Fig. 15 represents a "tripping type curve standard" for ideal and normal conditions. The first high peak, caused by the change from static from dynamic conditions, is not seen in Fig. 14 but still stated by Cordoso et al. (1995) and Mme et al. (2012). The discussion of which forces cause this signature is to be addressed later on.

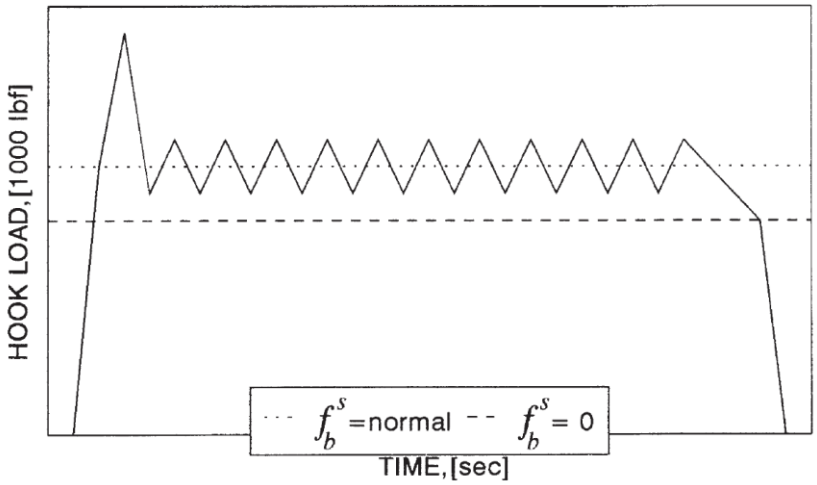

Figure 15: This graph is from Cordoso et al. (1995) which defines this as a "tripping type curve standard". The papers states that at the beginning and end of the operation, the acceleration effect predominates. Further it is stated that in the center third part the value oscillate around an average value.

4.2.2 Poor Hole Conditions

Poor hole conditions include among others:

- Tight hole
- Ledges
- Wash outs
- Poor hole cleaning
- Dog legs
- Key seats

All un-normal downhole conditions will affect the measured HKL, though differently in direction and also in magnitude. This report will limited itself to give examples and discuss generally how abnormal conditions will make the HKL deviate from the normal trend. For definitions and more detailed analysis of signature plots and diagnostic tools, reference is made to Cordoso et al. (1995) and Bjerke (2013).

Fig. 16 could be compared to Fig. 14 to see the difference between good and poor hole conditions during the tripping of one stand. These figures will be of importance when comparing the field data to the output of the mass – spring model and alternative model presented in this report.

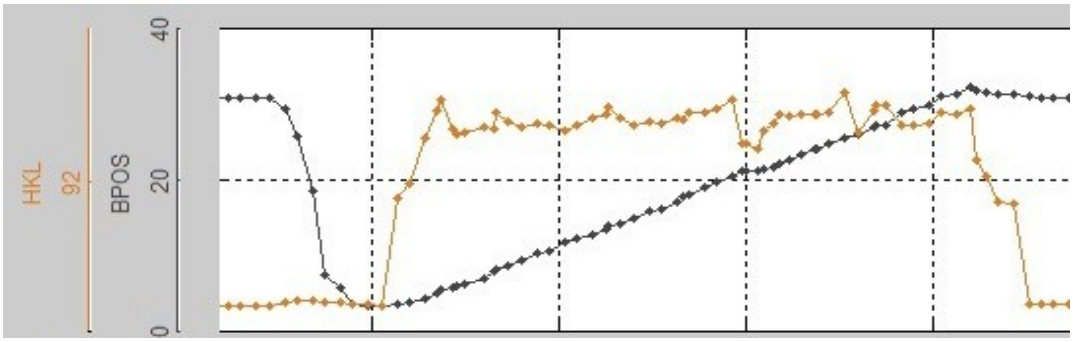

Figure 16: The figure shows a drill string being pulled out of a 17 ½" hole with a tripping speed of 0,16 m/s (3 min/stand) at 1950 mMD without circulation or rotation. The BPOS graph seems somewhat straight (but not as smooth as in Fig. 14), except for a relative long acceleration period. The HKL measurements are on the other hand not smooth compared to the ones seen during good hole conditions. This serves as an example of poor hole conditions (RTDD supplied by Statoil).

Fig. 17 shows another example from the given dataset. Some overpull is seen at the start of the interval, but then it follows a reducing trend (blue line), as anticipated. Suddenly a large overpull is seen (lowest red ring) and back-reaming out of the hole was necessary; the RPM and flow was turned on to start back-reaming.

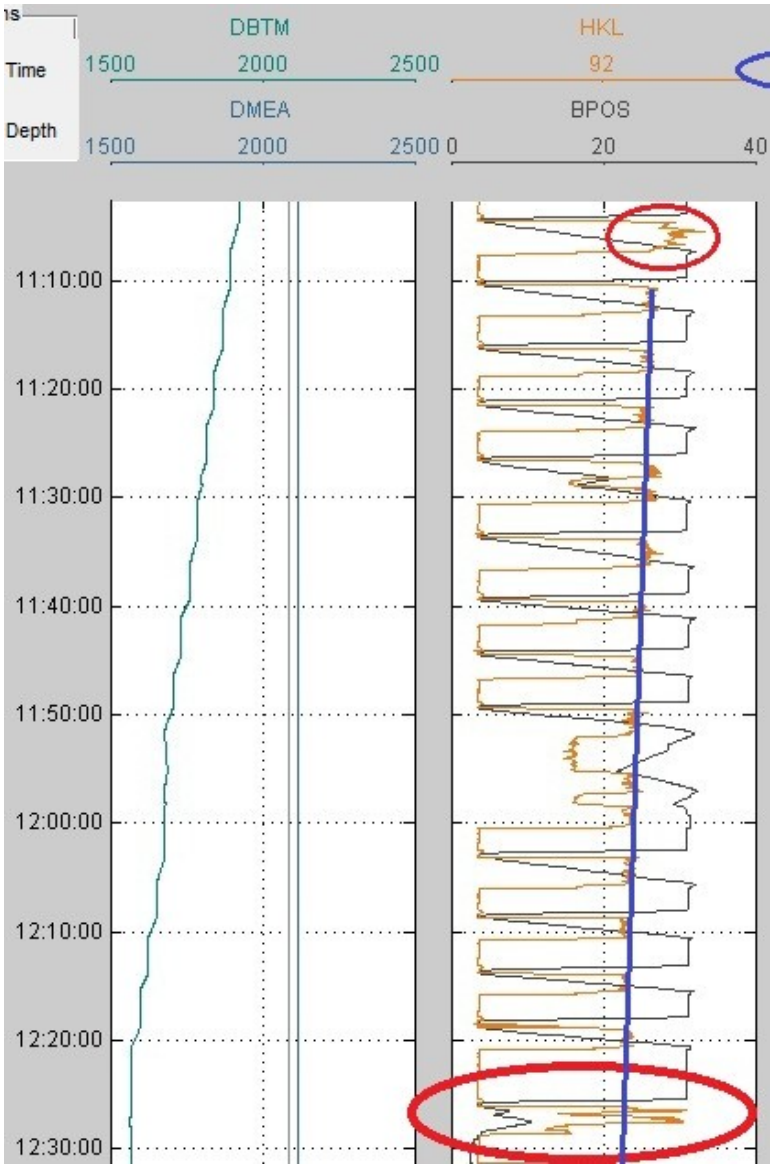

Figure 17: A 17 ½" hole tripped out taking 25 tons (EOW report 2007) overpull at 1563 mMD (lowest red ring). No circulation or rotation. The blue line shows the trend of the maximum experienced HKL during one stand over the interval. The overpull was encountered by back-reaming out of hole some 150 m. Note small spikes of a couple of tons at 11:30 and the red ring in top at 11:05. Was this a warning of the upcoming event? Note also the small spikes from 11:20 to 11:40 (RTDD supplied by Statoil).

5 Models

To accurately model the conditions and forces acting in the well is challenging. The complex behavior of many physical phenomena is not fully understood and is difficult to implement into a model. The complex modeling assembly developed at IRIS in Stavanger has managed to obtain good results with field cases (Cayeux et al. 2012a, 2012b; Cayeux and Daireaux 2009) and has avoided several instances of trouble and potential NPT (Cayeux 2012b). To reach the high standard quality of such global models, large amount of resources are invested.

The initial goal of this thesis was to investigate and to further develop the model presented by Mme et al. (2012), also shown in appendix D. The model is based on assuming that the drill string elements are connected by springs and then solve the force balance by numerical iteration along the well path. Due to difficulties in obtaining the needed expertise and experience with the background for the model, another angle of attack was chosen. As an introduction to the alternative model, the mass – spring model is presented in chapter 5.1 and the basis and structure are explained and comments are given. In chapter 5.2 the alternative model is presented and explained. The alternative model has been tested against field data.

5.1 The Mass – Spring Model

This sub-chapter will present the idea behind the mass-spring modeling concept and also the mathematical equations used in the MatLab script (appendix D). Most of the models trying to estimate the HKL parameter do it over several stands or average it to one value per stand. This model tries to model the behavior during the pulling of one single stand. The objective and purpose of doing so, is to try to be able to detect troublesome behavior at an earlier stage and thus initiate remedies faster than e.g. when doing trend analysis (ref. Fig. 17, Fig. 11, Fig. 10 and Fig. 9). Glomstad (2012) contained a similar mass-spring model and showed promising results when compared to laboratory experiments, although only during normal conditions and slow pulling speeds. During moderate and high speeds and non-ideal conditions, the model did not manage to simulate the behavior adequate. The laboratory experiments were conducted with a spring to imitate the elastic behavior of the drill string. The unpublished paper by Mme et al. (2012) compared the model to RTDD from a well in the North Sea. The

conclusion was that the model fits well with field measurements during normal conditions, but the weakness was a poor ability to model the acceleration effect at the start of the tripping operation. Also a lot of adjustments were needed to obtain reasonable results.

5.1.1 Concept and Model Input

The idea behind modeling the drill string as a spring is the elastic behavior of the material of which it consists. As exemplified by calculation in chapter 2.5 Inertia forces and Elastic Behavior, the string can elongate significantly when subjected to tension forces. A typical drill string is often a couple of times longer than the one used in the example calculation and the overpull might be up to as much as 90 tons, resulting in several meters of elongation.

Fig. 18 shows an illustration of how the mass-spring model works. Drill string elements are connected by springs and the forces and acceleration effects are integrated along the well path.

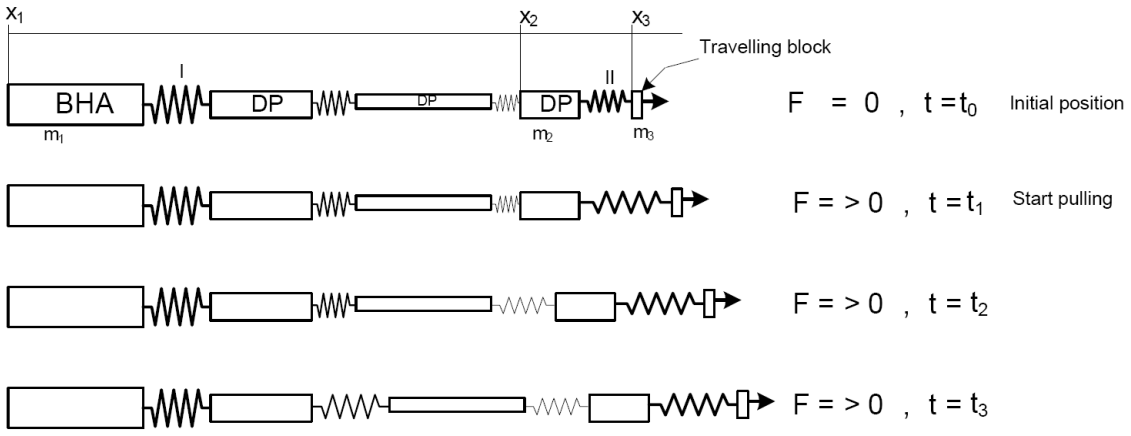

Figure 18: Illustration of mathematical model and spring concept of the mass – spring model (Mme et al. 2012).

To obtain the correct weight of the drill string, good estimations of the friction forces etc, input values from the field operation are needed. The only dynamic parameter in this model is the block position, BPOS, the other parameters are assumed constant during the pulling of one single stand. The next sub-chapters will describe the input parameters.

Mud Weight: As described in chapter 2.3.2 Buoyancy, the drilling fluid will reduce the effective weight of the submerged object, in this case the drill string. The buoyancy factor is typical in the range from 0,85 down to 0,75, thus reducing the weight from 15 to 25 % relative to weight in air. The assigned value in the model assumes a homogeneous fluid with no cuttings. This is a reasonable assumption due to the fact that the well most likely has been circulated before tripping out and due to the fact that there is no fluid circulation in the well when looking at the ideal situations.

Drill String Pipes: The only part of the drill string that is not made up of drill pipe, is the bottom hole assembly, BHA. Drill pipes are normally made of standard steel with a density of 7840 kg/m^3, and have a specified inner and outer diameter. This gives the volume of the pipes and together with the density, the weight is obtained. Some of the pipes might have some degree of wear and thus have a lower weight than the nominal one, but this error is not taken into account in this model. The input is thus the length of the BHA and the remaining part of the string is drill pipes.

Friction Factor: Without doubt, the FF is the single most uncertain parameter. As discussed in the theory chapter in this report, the friction factor is a function of many variables; rock type, degree of lubrication, contact points, static or dynamic conditions and so on. The mass-spring model differentiates between the static and dynamic conditions in trying to simulate the stretching and spring motion effects of the pipe. This is done by assigning a static friction factor and estimates the needed force to make the string moving. After the estimated force is surpassed, the model will switch to a dynamic FF. This is what results in the first high peak (to around 110 tons of HKL) in Fig. 19.

5.1.2 Mathematical Equations

The basic mathematical equations used to model the HKL behavior in the mass-spring model are:

$$m_1 \cdot a_1 = k_{12} \cdot (x_2 - x_1 - \Delta_{1-2}) - F_1 - F_{D1} \tag{26}$$

$$m_2 \cdot a_2 = k_{23} \cdot (x_3 - x_2 - \Delta_{2-3}) - k_{12} \cdot (x_2 - x_1 - \Delta_{1-2}) - F_2 - F_{D2} \tag{27}$$

$$m_3 \cdot a_3 = HKL - k_{23} \cdot (x_3 - x_2 - \Delta_{2-3}) - F_3 - F_{D3} \tag{28}$$

$$F = \beta \cdot g \cdot m \cdot (\cos\alpha + \mu \cdot \sin\alpha) \tag{29}$$

$$F_D = \frac{\pi \cdot d_s (dx) \cdot \mu_{\text{viscosity mud}} \cdot v}{d_h - d_s} \tag{30}$$

Here m is mass, a is acceleration, k is the spring constant, x is distance, Δ is the original distance between x_2 and x_1 when the spring is not stretched, F is weight and frictional force due to mechanical surface friction, F_D is fluidic drag due to viscous forces. Further; β is the buoyancy factor, α is the inclination angle, μ is the friction factor, $\mu_{\text{viscosity mud}}$ is the mud viscosity, d_h and d_s are the diameter of the hole and string respectively, v is the drill string velocity and (dx) is the distance travelled by the drill string element.

5.2 The Alternative Model

The assumption for the alternative model is that the forces acting on the drill string can be summarized in four main categories;

- Tension / compression
- Friction at steady state tripping
- Acceleration / retardation
- Other forces

The three first categories can be expressed according to Eq. (31);

$$HKL_{\text{model}} = \alpha \cdot \Delta l + \beta \cdot v + \omega \cdot a \tag{31}$$

Here HKL_{model} is the modeled hook load, Δl is the elongation of the drill string, v is the velocity forces, a is the acceleration forces and α, β and ω are empirical constants. The empirical constants are adjusted to best fit the measured HKL. When the optimal values of the constants are found, they can be used on the next stands of pipe being pulled. This way deviations or changes in the relationship between the three terms will indicate which forces are dominating. If the modeled HKL gives a good match during the normal conditions, any deviation between the modeled and the measured HKL can be interpreted as troublesome behavior.

The input values as well as the result values in this model are normalized to fit into a HKL interval from 0 to 1. The acceleration effect will be negative during the deceleration in the end phase of the tripping operation. The model is used as a tool to determine the relative magnitude of the three forces. When the values are normalized, the empirical constants should sum up to 1,0. Whenever the modeled values result in lower or higher values than the measured ones, there are other forces acting than those included in Eq. (31).

5.2.1 Stretch / Compression

The stretch or compression, denoted Δl, of the pipe is of significant importance in the total force suspended in the hook. In this model, the elongation is calculated

between the block position, BPOS, as the top end of the string, and the bit position, BitPOS is the lower end. These measurements are assumed reliable and accurate to calculate the length and thus the stretch of the drill string. Eq. (32) presents how the stretch is calculated. The minimum length of the string during the specific tripping operation is subtracted from the dynamic and constantly changing length of the string.

$$\Delta l = (BPOS + BitPOS) - \min(BPOS + BitPOS) \tag{32}$$

5.2.2 Friction at Steady State Tripping

The velocity, v, of the drill string affects the measured hook load. This especially applies to the viscous forces from the drilling fluids. As the velocity increases, the same does the viscous frictional forces since the shear stress, τ, is proportional to the drill string velocity. The velocity affect is calculated by input from the BPOS and sampling time, calculating the velocity of the string from the equation;

$$v = \frac{\Delta BPOS}{\Delta t} \tag{33}$$

5.2.3 Acceleration / Retardation

The force needed to accelerate the drillstring and the dead weight of the travelling block equipment is significant. The mass of the total string can be several hundred tons. According to Eq. (13) this results in a high force needed to make the drill string change its state of motion. The acceleration is calculated by the input of time and change in velocity by the equation;

$$a = \frac{\Delta v}{\Delta t} \tag{34}$$

6 Results

This chapter will present the results from both the mass – spring model and the alternative model. The results from the latter model were obtained during this report work while the mass – spring model results were found from Mme et al. (2012).

6.1 The Mass – Spring Model

Fig. 19 shows one of the results from the modeling preformed in Mme et al. (2012). The red and blue solid lines are field measurements, HKL and BPOS respectively. The dotted red line is the modeled HKL. As can be seen from the figure, the modeled HKL has a sharp initial increase in the acceleration phase but fails to simulate the less sharp increase in HKL seen in the measured data. The model almost manages to reach the high value of the initial peak in the measured data, but drops off too fast and does not catch the small dip seen immediately afterwards. After this, the average HKL values are simulated in an acceptable manner. The friction factor is set to fluctuate around a set value to imitate the small fluctuations in the field measurements.

The measured HKL signature shown in Fig. 19 shows remarkable similarities to Fig. 5 in chapter 2.4.5 Static and Dynamic Conditions. This might indicate that during the tripping of this stand, the change from static to dynamic friction is the predominating phenomenon.

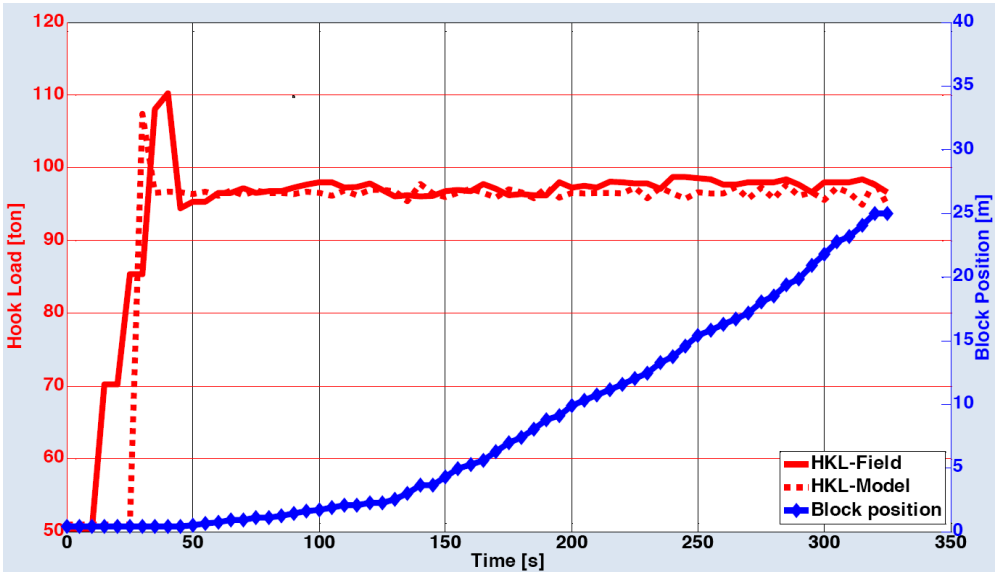

Figure 19: Result from testing of the mass-spring model against RTDD (Mme et al. 2012).

It can be seen from Fig. 19 that the sampling rate of which the field measurements were done, was of low frequency; approximately 1 sample per 5 seconds, giving a sampling rate of 0,2 Hz.

6.2 Alternative Model

This chapter will present the field cases that were selected for testing, the test procedure and the test results from the alternative model. The two stands that were selected for testing are shown in Fig. 20, named Stand 1 and Stand 2.

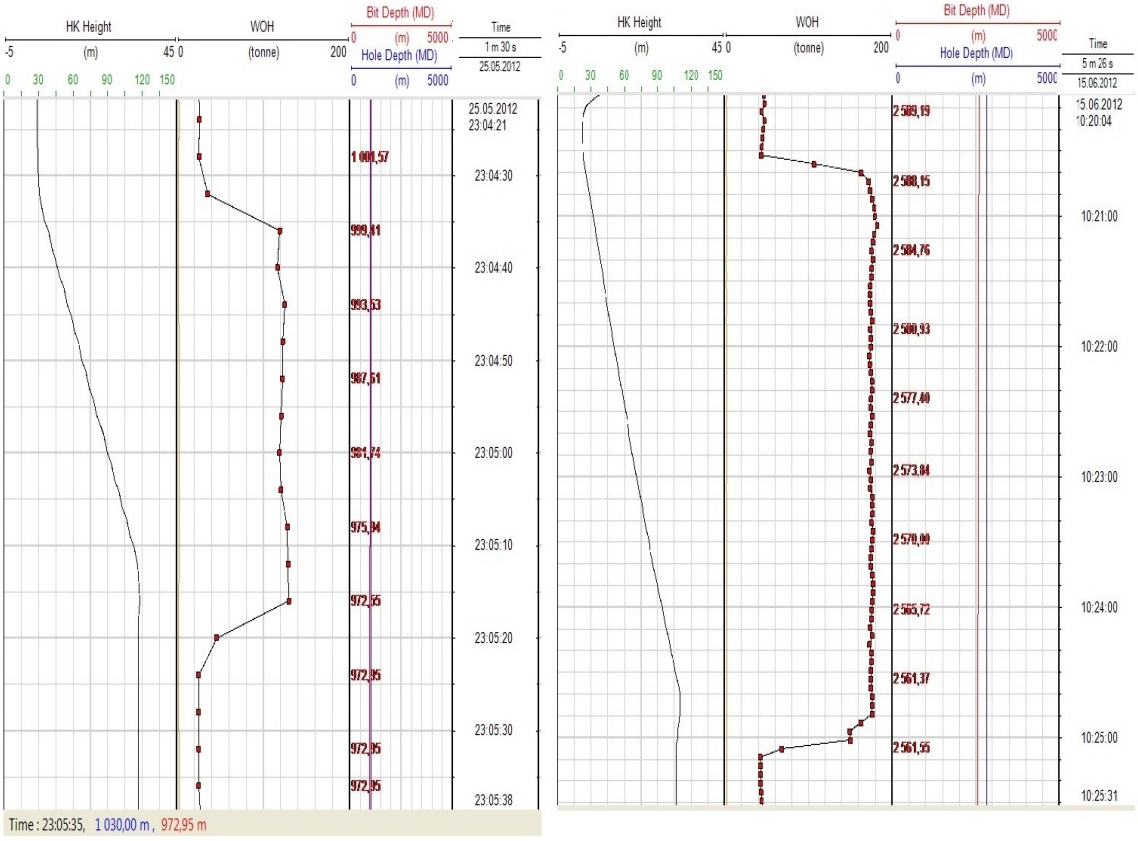

Figure 20: The original two stands selected for testing purposes. To the left is Stand 1 and to the right is Stand 2. The abbreviations HK and WOH are spelled out to Hook and Weight On Hook respectively. The red squares are the raw data sampling (Screenshot from Discovery Web™).

To observe how the different terms in Eq. (31) would affect the resulting modeled HKL, the simulations were performed with four sets of values for the empirical constants. In the three first runs, named Test α, Test β and Test ω (see Table 2 and Fig. 21), one of the constants were set to 1,0 while the others were set to 0,0. This was done to observe how the terms in Eq. (31) responded to the input field data.

Table 2: The test matrix showing the values of the empirical constants used in the simulation of the alternative model.

Test α α = 1,0 β = 0,0 ω = 0,0	**Test β** α = 0,0 β = 1,0 ω = 0,0
Test ω α = 0,0 β = 0,0 ω = 1,0	**Test Best Fit** α = best fit β = best fit ω = best fit

In the Best Fit test, the empirical constants were manually adjusted and fitted so that the modeled HKL curve gave the best match to the field measurement curve. The procedure that was used here was;

1. Set the constants α, β, ω = 1/3.
2. Observe the resulting simulated HKL.
3. Based on the graph obtained during 2., Test α, Test β and Test ω.
    a. Adjust the empirical constants and try numerous combinations of the empirical constants.
4. Note the values of the constants that give the best fit.

The two stands that were used as input to the alternative model are called Stand 1 and Stand 2. The imported field data is further explained and discussed in chapter 8.3

Imported RTDD and the complete tripping operations of the two cases are found in appendix C.

6.2.1 Stand 1

Stand 1 was a 100,57 mMD long string pulled out of a 17½" wide and 1030 mMD deep hole. The stand was pulled out of the hole at a high speed and showed no abnormal downhole indications. The raw data from Discovery Web™ are given to the left in Fig. 20 and in Appendix C. The modeling results are shown in Fig. 21.

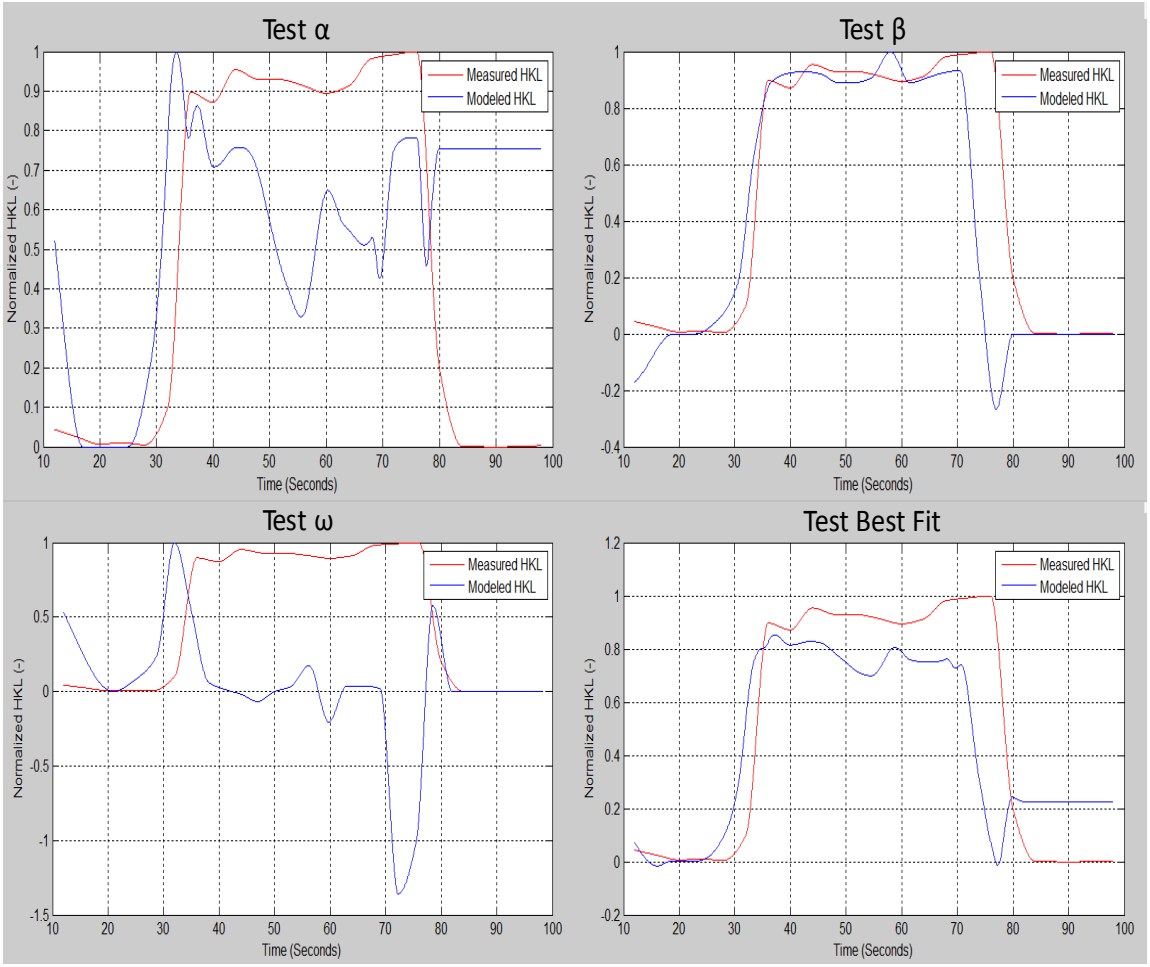

Figure 21: Stand 1 was a 100,57 mMD long string pulled out of a 17½" wide and 1030 mMD deep hole. Test results from isolating the three dominating forces α, β, ω, are shown in Test α, Test β and Test ω. Upper left has α = 1, upper right has β=1 and lower left has ω = 1. After numerous tries, the best fit was obtained by α, β, ω as 0,3, 0,65 and 0,05 respectively, shown at the lower right.

A first observation is that the modeled HKL, blue curve, seems to be shifted to the left compared to the red curve of the field measurements. The stretching effect, α=1 up to the left in Fig. 21 seems to be quite well modeled in the acceleration phase and the retardation phase. In the middle third part it seems to correlate to the changes in field measurements, but the amplitude from the model seems to be too high. The velocity

frictional effect, β = 1, seems to fit well on an average basis and value. On the other hand it does not match the peaks and other small changes during the pulling. Also it decreases a bit too early in the end. As anticipated, the acceleration, ω = 1, has its main amplitudes at the start and stop of the pulling. Just as the stretching effect, the acceleration seems to be shifted a bit to the left.

6.2.2 Stand 2

Stand 2 was pulled during typical normal conditions. The results from modeling the HKL with field data input are shown in Fig. 22. Bjerke (2013) used this stand as a good example of typical normal conditions and the stand follows the typical signature

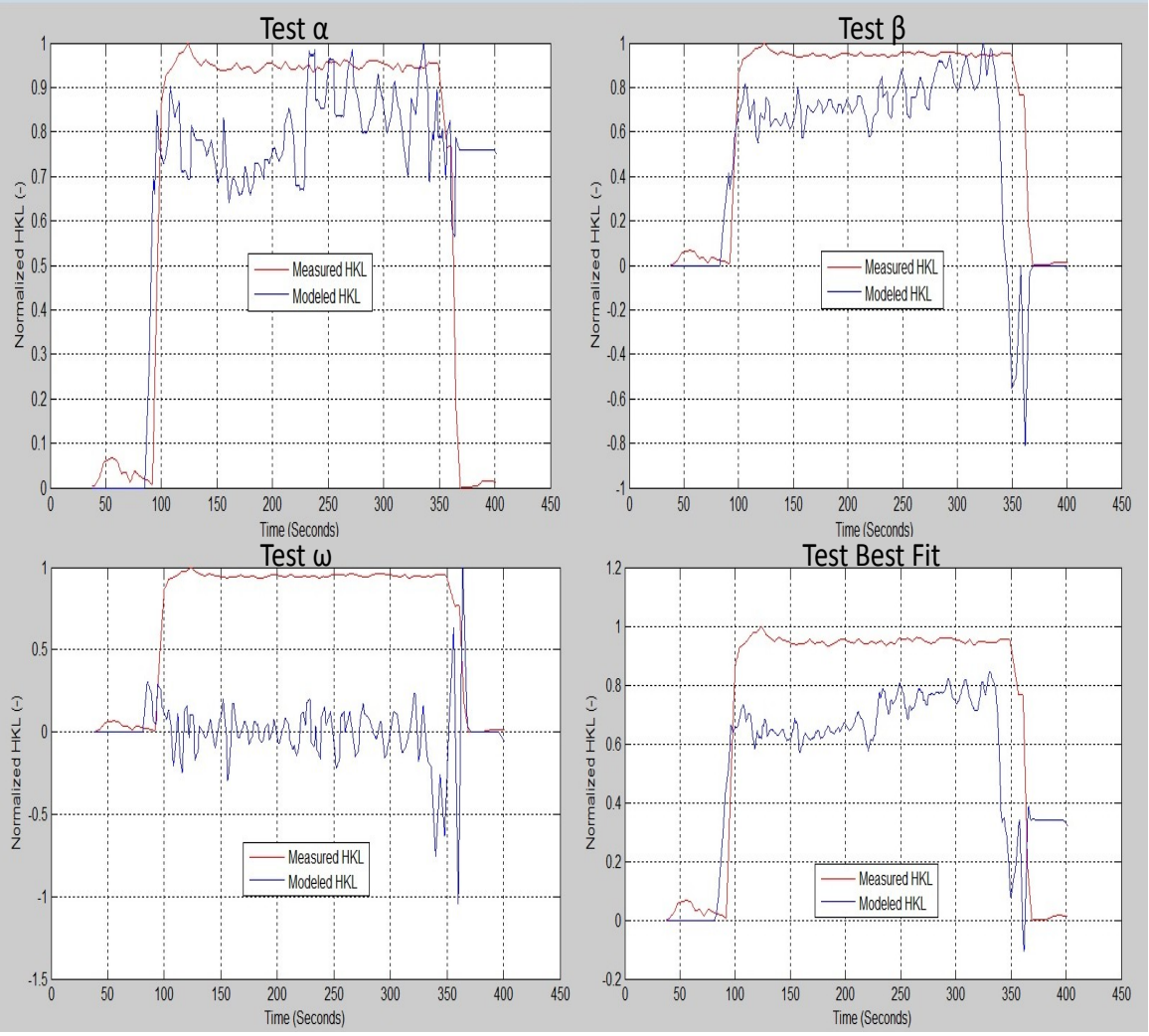

Figure 22: A 2 589,18 mMD long drill string was pulled out of a 2818,00 mMD long and 17 ½" wide hole. Test results from isolating the three dominating forces α, β, ω. Upper left has α = 1, upper right has β=1 and lower left has ω = 1. After numerous tries, the best fit was obtained by α, β, ω as 0,45, 0,45 and 0,10 respectively, shown at the lower right.

defined by Cordoso et al. (1995). The 2 589,19 mMD long drill string was pulled out of a 2 818,00 mMD long and 17 ½" wide hole. According to the drilling report, the drill string took 15 tons weight at 2 600 mMD. The operational team ran in hole below restriction and pulled through without further problems. The presented stand is the one following the restriction. This is interpreted as a good stand to test the model against slower pulling speeds and a longer string with more mechanical friction.

An improved interpolation method was used on the stand 2 and it seems that the left shifting of the model output compared to the field measurements is less evident. On the other hand, the results in Fig. 22, show little amplitude of the acceleration in the start of the pulling operation and high both negative and positive in the deceleration phase. This behavior was not anticipated and will be discussed in next chapter.

7 Evaluation of Results

The results from Mme et al. (2012) and from the alternative model-simulations in this report will be discussed and evaluated in this chapter.

7.1 The Mass – Spring Model

The results obtained by Mme et al. (2012) shown in Fig. 19, can be said to have both strong and weak points. The fluctuation around an average HKL value during the center part of the operation shows good correlation to the field measurements. The use of a set and fixed fluctuation assumes that friction in fact does fluctuate and change along the well path. A weak point here is that this is a pure mathematical manipulation to make the HKL imitate fluctuation. This is important to state and to be aware of. The source of the fluctuation behavior could be stick – slip behavior of the string along the path, accumulations of cuttings or other restrictions. This would make the string movement retarded and accelerated. Obviously, the fluctuation should have a physical source, not a mathematical manipulation.

On the other hand, both the stretching and acceleration of the drill string at the start of the tripping operation seem to be poorly matched. The modeled HKL increases rapidly without the "stair" signature seen in the field values (the "stair"-phenomenon is discussed in chapter 8.3.2). The modeled values also decrease more rapidly than the measured ones and do not manage to show the spring effect after the first high peak (seen as a decrease in the field measurements). Mme et al. (2012) give examples of a direct relationship between the acceleration of the BPOS and HKL measurements gathered from field operation. This implies that the model needs improvements to show this effect.

7.2 The Alternative Model

Overall, the alternative model gives lower estimated HKL values than the field measurements. This would directly insinuate that there are forces of significant magnitude present and that are not included in the model. The improved interpolation method seems to reduce the left - shifting of the modeled HKL. On the other hand, Stand 1 correlates better to the RTDD than Stand 2.

7.2.1 Stand 1

Overall, the results of the isolated Test α, Test β and Test ω fit somewhat with the expected results. In the start of the tripping operation, all the forces are increasing and contributing to a first high peak. Especially the stretching and acceleration term seems to develop as expected; increasing in the start phase and reducing in the retardation phase. The friction during steady state friction also seems to correlate well with the anticipated behavior; a smooth and stable value during the constant velocity period and reducing in the end. The negative value (- 0,2) in Test β is an interesting observation. This would indicate that the drill sting moves down the hole, but by taking a look at the RTDD in Fig. 20 and in Appendix C, this shows a lowering of the block. This is well in accordance with the procedure when the drill string is put in slips after the tripping operation is completed, and is thus correct.

The final, manual fitted Test Best Fit, does not show as good match as hoped. Some curves and behavior are similar, but the overall impression is that it is not sufficient accurate to be able to detect troublesome behavior in the well.

The left – shifting seen in Fig. 21 is believed to be caused by the interpolation method. This is supported by the fact that it is less evident in Stand 2.

7.2.2 Stand 2

The first thing to observe from Fig. 22 is that the interpolation method seems to have fixed the left - shifting of the modeled results compared to the measured values. The next thing to notice is that this Stand 2 also has an overall lower HKL than the RTDD and that there thus are other forces involved than the ones included in Eq. (31). This stand is pulled at a much lower speed and thus has a larger number of raw data measurement points, giving a more detailed graph. It is seen that both the field data and the model output is much sharper. Even though the RTDD shows a relative straight line in the steady state phase, the modeled HKL shows large amplitudes. The reason for this is that the equations in the model have a high sensitivity for changes in the RTDD. And since the RTDD has a low resolution in time space, this would lead to large amplitudes in the model output.

The tension / compression effect is difficult to correlate to the RTDD and shows a poor match. The friction during steady state tripping shows an increasing trend during the whole operation. This is not found in the RTDD.

8 Evaluation of Report, Models and Data

The two models presented in this report have their strong sides and their weaknesses. The basis of the mass – spring model is physical relationships expressed in mathematical equations solved by numerical integration along the well path. Thus this model is rooted in equations describing the physical nature of the conditions in the hole. This is a good foundation for further development of a trustworthy way to estimate the needed force to pull the string out of the hole. On the other hand, by investigating the model further, it has its weaknesses. These are addressed in the coming sub-chapters.

The alternative model is on the other hand, not based on well known and accepted physical relationships of friction, fluid viscosity and dimensions of the involved equipment. It is rather a way to identify the dominating forces affecting the force to pull the pipe, and the relative magnitude between them during the different phases of the tripping operation.

8.1 Quality of Mass – Spring Model

The presented model gives basic descriptions of the physical effects influencing the force needed to move the pipe in the hole. Personal communication with Eric Cayeux at IRIS in Stavanger has provided the author with valuable information with respect to the relationship between the theoretical modeling and the physical operational procedure. Some of the important topics are presented and discussed below, based on this communication.

HKL vs. Top of String Force: The hook load force needed to move the string in the hole is in most cases calculated by estimating a "top of string force"; the weight and force from the hook and down into the hole. As discussed in chapter 2.2 Rig Set Up – HKL Sensor, there are several sources of error in the measurement equipment. Between the point where the reported HKL values are measured and the "top of string", there is often an arrangement of equipment including the hoisting assembly, several wires of drill line, a top-drive, mud hose etc. According to Cayeux[9]; "the assumption

[9] Personal communication with E. Cayeux (Chief Scientist). 2012. Stavanger: IRIS (International Research Institute of Stavanger.

that this equipment is a constant weight that is added to the top of string force is largely erroneous!" This equipment might contribute, or even be the source of, physical phenomena registered in the HKL measurements. This should be further investigated and included if showed to be correct.

Mud Weight: The density of the mud influences the uplifting buoyancy force. A denser fluid will reduce the effective weight of the drill string pipes. The density of the drilling fluid that is put into the well is regularly checked by the operational rig team. The mud density is of critical importance in terms of well control. It is measured and checked both when going into and out of the well, but there are physical parameters affecting the local density. The most important ones are;

- Pressure
- Temperature
- Additional constituents such as gas and cuttings

The effect of changes in the pressure and temperature again depends on the compressibility and thermal expansion of the drilling fluid. This introduces the need for PVT-calculations to make accurate predictions of the mud density which in turns depend on temperature estimations.

Another aspect in buoyancy estimation is the presence of mechanical equipment like float subs. This kind of equipment prohibits the inflow / backflow of fluids into the drill string. This is especially important when tripping into the hole and requires the need for filling the drill string with mud from the top. On the way out of the hole, the fluid might not be able to flow back into the hole, and the drill string might be filled all the way to the top. Also the drill string which is above the drill floor and top of the mud fluid surface will not experience any buoyant force.

Drill String Pipes: Assuming that the pipes making up the drill string still have their nominal and fabricated dimensions is not a good one to make. Still, this is usually the case when torque and drag calculations are done. The pipes will wear, both on the outside as well as the inside (!), influencing the estimated weight of the pipes to a significant degree. The inside wear on the pipes are supported by experiencing lower stand pipe pressures than expected, due to lower pressure loss in the drill string. Due to this Cayeux et al. (2012 a) express the importance of correct and detailed calibration of any model. The mass – spring model does not include a calibration sequence neither the

ability for the user to specify the dimensions of the pipes. The model would benefit from having this implemented.

Friction Factor: By using this kind of approach, the conservative coulomb friction estimation, the friction factor accounts for all the effects that are not included in the model. The fudge term is certainly valid as an adjective to describe the FF. This is important to be aware of, if the obtained FF is to be compared to similar wells or operations which do not have the same effects included in the model. This obviously applies to all friction estimation models. To be able to compare results and friction factors between different software outputs, it should be understood what assumption that are made and what it includes.

Mathematical Equations: The mathematical equations used in this model are of simple character compared to other more complex models present, e.g. DrillScene and Drill Tronics developed at IRIS, where the well is considered global and equations are interconnected. On the other hand, using a spring concept as the point of departure is interesting and might better be able to model the acceleration behavior. An essential thing in using this concept is the need to know where the drill string is in contact with the borehole wall. This again requires accurate information about the well path and deviations from the planned, smooth and optimized path.

The model assumes that under normal ideal conditions, there will be a "first high peak" that is assumed to be the switch from static to dynamic conditions. Based on established and accepted physical principles, as presented in chapter 2.4 Friction, the switch from static to dynamic conditions could be significant if the conditions are considered as "dry friction". If it, on the other hand, is considered as lubricated friction, the smooth change from static to dynamic (ref. Fig. 14) could be the case. The signal plot can in that case be used as a diagnostic tool to evaluate the lubricating effect of the mud in the well and the first high peak could be a restriction rather than switch from static to dynamic movement. These are questions not addressed in the unpublished paper, or in the model itself. The assumption that it in fact is the transition from static to dynamic conditions is supported by Cordoso et al. (1995). On the basis on the work done in relation to this thesis, the author is not convinced that it is so. Among things to

support this skepticism is Fig. 14. This is a long string that should have significant amounts of mechanical friction holding it back, but the first high peak does not occur.

Other Factors: The main and most important subjects affecting the measured HKL are mentioned in the above sub-chapters. Among other things that could be taken into account are the rig type and weather conditions. The use of a floating drilling installation requires methods and equipment that reduces or almost eliminates the heave motion of the rig relative the drill string. In most cases the effect is not completely removed. Cespedes (2012) modeled the heave motion with a numerical model and concluded that the drill string certainly is affected by the heave motion and that the bottom movement differs from the forced movement at the top, due to drill string elasticity.

8.2 Quality of Alternative Model

The idea behind the alternative model was to be able to point out a set of values for the empirical constants and then use them as a definition of normal behavior relative the specific well and the specific equipment used (e.g. rig type, drilling equipment, hoisting equipment. etc.). This idea could be said to be a kind of calibration. The strong point of this model is that it is simple and does not require detailed knowledge about the operational equipment used. It defines some parameters to be normal and then use them as a definition to detect deviation from normal. The fact that it normalizes the values, adds the benefit of comparing the effects to each other. From the test results, the model seems to be able to simulate some of the dominating forces in a sufficient way, especially when tested against Stand 1.

The obvious weak spot is that it is not based on detailed physical relationships between the involved materials and forces. The model also seems to have a high sensitivity of the input parameters. This high sensitivity is in fact a good sign. If the troublesome conditions occur, the model output would give even higher amplitudes, thus give even stronger indications of poor conditions. The model is not consistent in units and thus can be said to not have a solid physical foundation.

8.3 Imported RTDD

The field measurements used in the alternative model were accessed through Statoil's database Discovery Web™. The initial requirements for the selection of the stands were;

- The drill string should be relative short
- No indications of abnormal well conditions
- No circulation
- Fast pulling speed

These requirements were set to have simple test conditions and model a drill string that did not have significant portions of mechanical friction involved. The fast pulling speeds were required to check if the model would be able to estimate the magnitude of the acceleration effect without too much dampening friction. After Stand 1 was tested, also a longer string at low pulling speed was modeled. This could reveal potential weaknesses and points where it would be valid for both situations.

Data Sampling Rate and Interpolation: The field data used in this case study was acquired by different service companies on the behalf of Statoil. The sampling rate of which the parameters were recorded and made available in the database was almost constant but varied around 0,2, and at times up to 1 Hz. Also the different parameters had different sampling rate and time of sampling. The parameters were given with a time accuracy of per second. By investigating e.g. the BPOS measurements and communicating with a driller in the North Sea, the shape of the BPOS showed in most cases a strange behavior. Fig. 23 shows an example of both uneven and inconsistent sampling rate.

Cordoso et al. (1995) stated that the needed sampling rate to be able to catch the acceleration effects was around 3 Hz. After contact with the responsible people in Statoil, it became clear that it was not possible neither with a higher sampling rate nor a more accurate and specific time of sampling (e.g. in tenths of a second). Taking a look at Eq. (33) and Eq. (34), it can be seen that even small changes in time would cause large differences in the calculated parameter. If the goal is to accurately model the parameters including forces such as acceleration and elastic effects, it would definitely be beneficial, or even essential to deal with measurements and data with a higher sample frequency. This is supported by Cordoso et al. (1995).

Stair Phenomenon: The "stair" phenomenon, illustrated both in Fig. 19 and Fig. 23, is important to know the cause of. This behavior is not seen on the rig[10] and do not have an intuitive background. The speed of the block is best of at a constant speed. Analysis and discussion about this has resulted in the belief that this is caused by the round off of the measured values and that the recorded parameters are put in the "nearest second", since the resolution in the time space is in number of seconds. This could result in values being put quite significantly away from where they should have been. If this is the case an increase in the resolution in the time space to around 1/10 of a second would eliminate the problem, or at least state if this is the cause or not. In the interpolation, this was assumed to be correct and measurements causing the stair tendency were removed from the dataset.

Figure 23: Illustration of uneven sampling rate as well as inconsistent rate. This phenomenon excluded several stands to be used in modeling. The purple upper ring shows two raw data points with a sampling rate of 0,2 Hz, the blue and green rings show data points with 1 Hz sample rate and the lower purple ring shows a frequency of 0,5 Hz. Also the "stair" phenomenon is seen in this figure; a steeper slope is observed when the sampling rate is higher; green ring compared to lower purple.

[10] Personal communication with Ronny Isaachsen, Driller, 2013. Ocean Rig.

8.4 Future improvements

During this report work, both investigating the mass – spring model from Mme et al. (2012) and the testing and analysis of results from the alternative model, the author would recommend some points to the checked and further developed.

Sampling Rate: When the goal is to be able to model and imitate parameters measured in the field, it is of crucial importance to know how the parameters actually develop and behave in the first place. This report has aimed to be able to model the tripping of a stand of drill pipe. To do so, there are mechanisms that change and interact in a very short interval of time, e.g. the acceleration effect. The field measurements used in this report had a sampling rate from 0,2 Hz to 1Hz. Supported by Cordoso et al. (1995), it would be recommended to acquire field measurements with a sampling rate of no less than 3 Hz. This would most likely give a more detailed picture of how the parameters change and develop as well as act as an aid to better understand the forces involved. Also a consistent sampling rate would be beneficial for interpolation purposes, since the time interval is fixed.

The Mass – Spring Model: The assumption that the first high peak is caused by the change from static to dynamic conditions should be investigated further. Is this the case, then the idea of using two friction factors in the mathematical model could give additional information. If the model is tuned, calibrated and matches the field data, the static and dynamic friction factors can be stated and act as a input for calculation purposes for other operations in the well.

The model would benefit from implementing estimations of the contact points between the drill string and the walls of the hole. Since the model aims to treat string elements as mass points connected by springs, the location of the dampening friction is essential to know.

By assuming that the other parameters influencing the HKL are static, potential errors are introduced, like discussed in previous sub-chapters. To include them as dynamic inputs would require much resource and might not be defensible. It might be best to continue to treat them as static inputs.

The Alternative Model: Through, the alternative model has been attempted to use information from the RTDD and the relationships between the measured parameters to simulate the behavior of the field HKL. The goal has not been to make a model to simulate the absolute values of the field HKL, but rather a way to compare the involved forces and detect at which stages of the tripping process they are dominating. For the model to manage to reach this goal, further improvements are needed.

The use of the BitPOS as an input to the model would reveal the stretching and compression of the drill string. However, it is now understood by the author that BitPOS is not a measured parameter, but estimated on the basis of BPOS. The estimation of BitPOS will have to model stretching and compression of the string. This would in fact be a good problem to investigate further in a thesis for coming students. The challenge would be to create the solution to this problem.

The fact that the alternative model does not have a physical foundation makes it less trustworthy. The terms presented in Eq. (31) should be investigated and sources of error should be analyzed. If the model shall be used as a foundation for further development, an idea could be to split the tripping operation into three intervals; acceleration, steady state and retardation. In these three intervals, the empirical constants could change their values to more correctly imitate how the forces dominate each other in the different phases.

For further development of the model, more case studies should be conducted, preferable tested against field measurements with a sampling rate of at least 3 Hz.

8.5 Practical Application

It is well known to the petroleum industry that drilling wells is an expensive operation and that reducing the NPT has large cost saving potential. The idea of using RTDD to continuously update well models has proved to be beneficial (Cayeux et al. 2012a, 2012b) to avoid troublesome conditions. The presented models aim to detect the potential trouble before it evolves, so that remedies can be recommended. The mass – spring model aims to estimate the actual force needed to pull the string out of the hole. This is both complex and difficult to achieve.

When the alternative model has reached its potential, it can be used as a tend analyzer and trouble analyzer (as shown in Fig. 9, 10 and 11). It defines normal conditions on the basis on the specific well and equipment used on the specific well. This differs from the conventional trend analysis since it focuses on each stand rather than over several stands of operation.

The procedure of using the alternative model in field applications would be like the following;

1. Detect normal conditions.
2. Make a best fit of the modeled values to the measured field data.
3. Note the empirical constants and define them as normal conditions.
4. Observe if the measured HKL values start to differ from the modeled HKL
    a. If they differ, there are changes in the hole and these can be investigated by changes in the empirical constants.
    b. If they don't; the well conditions are stable.

The author believes that both methods have the potential of detecting evolving trouble, but both methods need improvement and further testing.

9 Conclusion

The initial goal of this thesis work was to understand, investigate and further develop the mass – spring model (Mme et al. 2012), to better be able to estimate the force applied to the hook to pull the string out of the hole. During this work, the author and his collaborators were not able to further develop the MatLab model. Therefore another path was chosen and the alternative model was developed. The alternative model was then tested against field data, Stand 1 and Stand 2. After exposing the two models to field measurements, these conclusions could be drawn;

- To be able to achieve more trustworthy model outputs that match RTDD with input from field equipment, there is a need for complex and detailed physical modeling.

- The mass – spring model needs improvement in the modeling of the acceleration effect at the start of the tripping operation. If this is achieved it is reasonable to assume that the model has potential to detect troublesome behavior when applied to live drilling operations.

- The alternative model has proven its ability to match field data, but not in all aspects and will need further improvements to be a useful trouble detector. After further development along the ideas put forward in this report, it will become a valuable tool for detection of evolving troublesome situations.

- To better identify acceleration effects in field measurements, a sampling rate of at least 3Hz is necessary.

Nomenclature

Abbreviation	Description
BHA	Bottom Hole Assembly
BitPOS	Bit Position
BPOS	Block Position
CoF	Coefficient of Friction
DS	Drill String
FF	Friction Factor
HK	Hook
HKL	Hook Load
HS	Hole Size
ID	Inner Diameter
LPM	Liters Per Minute
LWD	Logging While Drilling
MWD	Measurements While Drilling
MD	Measured Depth
NPT	Non- Productive Time
OBM	Oil Based Mud
OD	Outer Diameter
POOH	Pull Out of Hole
RIH	Run In Hole
RPM	Rotations Per Minute
RTDD	Real Time Drilling Data
T&D	Torque & Drag
WBM	Water Based Mud
WOB	Weight On Bit
WOH	Weight On Hook

Parameter	Primary	Secondary
A	Area	
a	acceleration	
d	diameter	
(dx)	distance travelled by drill string element	
E	Young's modulus	
e	sheave efficiency	
F	force	
g	gravity constant	
k	spring constant	
m	mass	
n	number of sheaves	counter
t	time	
v	velocity	
W	weight suspended in the hook	
w	unit weight of a drill string element	
x	distance	
Δl	stretch, elongation of drill string	

Symbol	Primary	Secondary
α	azimuth	empirical constant
β	buoyancy factor	empirical constant
ρ	density	
ω	empirical constant	
μ	friction factor (FF, CoF)	fluid viscosity
θ	inclination angle	
τ	shear stress	
σ	stress	
ε	strain	

Subscript	Primary	Secondary
A	axial	
cs	cross section	
d	fluidic drag	
dl	deal line	
f	friction	
h	hole	
k	kinetic	
N	normal	
n	counter	
s	static	string
t	tension	time
pipe	drill pipe	
yp	yield point	
ys	yield strength	

References

Aadnoy, B.S., Fazaelizadeh M. and Hareland, G. 2010. A 3D Analytical Model for Wellbore Friction. *Journal of Canadian Petroleum Technology* **49** (10): 25-36.

Aadnøy, B.S. and Andersen, K. 2001. Design of Oil wells using analytical friction models. *SPE Petroleum Geoscience and Engineering* 32: 53-71.

Aadnøy, B.S., Larsen, K. and Berg, P.C. 1999. Analysis of Stuck Pipe in Deviated Boreholes. Paper SPE 56628 presented at the SPE Annual Technical Conference and Exhibition, Houston, Texas, 3-6 October.

Andrew, W., Hareland, G. and Fazaelizadeh, M. 2011. Torque & Drag Analysis Using Finite Element Method. *Journal of Canadian Petroleum Technology* **5** (6): 13-27.

Best, B., 1990. Lessons for Cryonics from Metallurgy and Ceramics, http://www.benbest.com/cryonics/lessons.html (accessed 6 May 2013).

Best Practice Drilling Operations; Quick Reference Guide, Statoil, revision 2, December 2008.

Bjerke. H. 2013. Hook Load Signatures Revealing Causes of Restrictions. MS thesis, Norwegian University of Science and Technology (NTNU), Norway (June 2013).

Bourgoyne, A.T., Chenevert, M.E., and Millhein, K.K. 1986. *Applied Drilling Engineering*, Vol. 2, 5. Richardson, Texas: Textbook Series, SPE.

Cayeux, E., Daireaux, B., Wolden Dvergsnes, E. et al. 2012a. An Early Warning System for Identifying Drilling Problems: An Example From a Problematic Drill-Out Cement Operation in the North Sea. Paper IADC/SPE 150942 presented at IADC/SPE Drilling Conference and Exhibition, San Diego, USA, 6-8 March.

Cayeux, E., Daireaux, B., Wolden Dvergsnes, E. et al. 2012b. Early Symptom Detection Based on Real-Time Evaluation of Downhole Conditions: Principles and Results from several North Sea Drilling Operations. Paper SPE 150422 presented at the SPE Intelligent Energy International, Utrecht, The Netherlands, 27-29 March.

Cayeux, E. and Daireaux, B. 2009. Early Detection of Drilling Conditions Deterioration Using Real-Time Calibration of Computer Models: Field Example from North Sea Drilling Operations. Paper SPE 119435-MS presented at the SPE/IADC Drilling Conference and Exhibition, Amsterdam, The Netherlands, 17-19 March.

Cespedes M. 2012. Heave effects on Drill String during connections. MS thesis, Norwegian University of Science and Technology (NTNU), Norway (Spring 2012).

Christophersen, L., Gjerde, J. and Valdem, S.2007. Final Well Report, Drilling and Completion, 34/10-C-47. Doc. No GF RESU-HF-06 00070. Statoil, Norway (April 2007).

Cordoso, J.V., Maidla, E.E. and Idagawa, L.S. 1995. Problems Detection During Tripping Operations in Horizontal and Directional Wells. SPE Drilling & Completion **2** (10): 77-83. SPE-26330-PA.

Dangerfield J.W. 1987. Analysis Improves Accuracy of Weight Indicator Reading. *Oil & Gas J.* **85** (32): 70-74.

Elert, G. 1998. The Physics Hypertextbook. http://physics.info/friction/summary.shtml (accessed 1 November 2012).

Falconer, I.G., Belaskie, J.P. and Variava, F. 1989. Applications of a Real Time Wellbore Friction Analysis. Paper SPE 18649 presented at SPE/IADC Drilling Conference, New Orleans, USA, 28 February - 3 March.

Fendley, P. 2001. University of Virginia. Physics, http://rockpile.phys.virginia.edu/arch6.pdf (accessed November 2 2012).

Florence, F. and Iversen, F. 2010. Real-Time Models for Drilling Automation: Equations and Applications. Paper IADC/SPE 128958 presented at the Drilling Conference and Exhibition, New Orleans, USA, 2-4 February.

Glomstad, T.S. 2012. Analysis of Hook load Signal to reveal the Causes of Restrictions. MS thesis, Norwegian University of Science and Technology (NTNU), Norway (June 2012).

Hart, R., 2013. Tufts University Center for Engineering Education and Outreach, http://www.ceeo.tufts.edu/robolabatceeo/coolandnew/Rob_HTML/StaticAndKineticFriction_HTML/Static-Kinetic%20Friction.html (accessed 6 May 2013).

Ho, H-S. 1988. An Improved Modeling Program for Computing the Torque and Drag in Directional and Deep Wells. Paper SPE 18047 presented at the 63rd Annual Technical Conference and Exhibition, Houston, USA, 2-5 October.

Johancsik, C.A., Friesen, D.B. and Dawson, R. 1984. Torque and Drag in Directional Wells – Prediction and Measurements. *Journal of Petroleum Technology* **36** (6): 987-992. SPE-11380-PA.

Kristensen, E. 2013. Field and Experimental Investigation of Hook Load. Project report, Norwegian University of Science and Technology (NTNU), Norway (January 2013).

Kucs, R., Spöker, H.F., Thonhauser, G., Zoellner, P. 2008. Automated Real-Time Hookload and Torque Monitoring. Paper IADC/SPE 112565 presented at the IADC/SPE Drilling Conference, Orlando, USA, 4-6 March.

Luke, G.R. and Juvkam-Wold, H.C. 1993. Determination of True Hook Load and line Tension under Dynamic Conditions. SPE Drilling & Completions **8** (4): 259-264. SPE-23859-PA.

Maidla, E.E. and Wojtanowicz, A.K. 1990. Laboratory Study of Borehole Friction Factor With a Dynamic-Filtration Apparatus. SPE Drilling Engineering **5** (3): 247-255. SPE-18558-PA.

Mason, C.J. and Chen, D.C-K. 2007. Step Changes Needed to Modernize T&D Software. Paper SPE/IADC 104609 presented at the SPE/IADC Drilling Conference, Amsterdam, The Netherlands, 20-22 February.

McCormick, J. and Liu, G. 2012. Torque and Drag Modeling Advanced Techniques and Troubleshooting. Paper SPE 156945 presented at the Annual Technical Conference and Exhibition, San Antonio, USA, 8-10 October.

McLaren, G., Hayes, M.J.S, Brown, N.M. et al. 2007. Improving the Value of Real-Time Drilling Data To Aid Collaboration, Drilling Optimization, and Decision Making. Paper SPE 110563 presented at the Annual Technical Conference and Exhibition, Anaheim, USA, 11-14 November 2007.

Mitchell, R.F. and Samuel, R. 2007. How Good is the Torque-Drag Model? Paper SPE/IADC 105068 presented at the SPE/IADC Drilling Conference, Amsterdam, The Netherlands, 20-22 February.

Mirhaj, S.A., Kaarstad, E. and Aadnoy, B.S. 2011. Improvements of Torque-and-Drag Modeling in Long-Reach Wells. Modern Applied Science **5** (5): 10-28.

Mirhaj, S.A., Fazaelizadeh, M., Kaarstad, E. et al. 2010. New Aspects to Torque-and-Drag Modeling in Extended-Reach Wells. Paper SPE 135719 presented at the Annual Technical and Exhibition, Florence, Italy, 19-22 September.

Mme, U., Skalle, P., Johansen, S.T. et al. 2012. Analysis and modeling of normal hook load response during tripping operations. Technical report, Norwegian University of Science and Technology (NTNU), Norway (unpublished).

NASA SP-8063. Space Vehicle Design Criteria; Lubrication, Friction, and Wear. 1971. Hampton, Virginia, USA: NASA SP-8063.

Niedermayr, M., Pearse, J. and Banks, M. et al. 2010. Case Study—Field Implementation of Automated Torque-and-Drag Monitoring for Maari Field Development. Paper IADC/SPE presented at the IADC/SPE Drilling Conference and Exhibition, New Orleans, USA, 2-4 February.

Nybø, R. 2009. Efficient Drilling Problem Detection: Early fault detection by the combination of physical models and artificial intelligence. PhD dissertation, Norwegian University of Science and Technology (NTNU), Trondheim, Norway (September 2009).

Occupational Safety & Health Administration (OSHA), United States Department of Labor. 2010. Drilling; Tripping Out/In, http://www.osha.gov/SLTC/etools/oilandgas/drilling/trippingout_in.html#set_slips (accessed 26 November 2012).

Rae, G., Lesso, W.G. and Sapijanskas, M. 2005. Understanding Torque and Drag: Best Practices and Lessons Learnt from the Captain Filed's Extended Reach Wells. Paper SPE/IADC 91854 presented at the SPE/IADC Drilling Conference, Amsterdam, The Netherlands, 23-25 February.

Schlumberger. 2012. Hook Load, http://www.glossary.oilfield.slb.com/en/Terms.aspx?LookIn=term%20name&filter=hook+load (accessed 2 December 2012).

Schooley, F. 2008. Weight Indicators – The downhole Eyes and Ears of the Operator. Well Servicing, July/August.

Sheppard, M.C., Wick, C. and Burgess, T. 1987. Designing Well Paths To Reduce Drag and Torque. *SPE Drilling Engineering* **2** (4): 344-350. SPE-15463-PA.

Skalle, P. 2011. *Drilling Fluid Engineering*, first edition. Ventrus Publishing ApS.

Skalle, P., Backe, K.R., Lyomov, S.K. et al. 1999. Microbeads as Lubricant in Drilling Muds a Modified Lubricity tester. Paper SPE 56562 presented at the SPE Annual Technical Conference and Exhibition, Houston, USA, 3-6 October.

Vos, B.E. and Reiber, F. 2000. The Benefits of Monitoring Torque & Drag in Real Time. Paper IADC/SPE 62784 presented at the IADC/SPE Asia Pacific Drilling Technology, Kuala Lumpur, Malaysia, 11-13 September.

Xie, L., Moran, D., Yan, L. et al. 2012. Sophisticated Software Analysis System and Use of Torque/Drag Modeling for Complex Well Operations Increase Operational Efficiency. Paper SPE 152056 presented at the Western Regional Meeting, Bakersfield, USA, 21-23 March.

Appendices

A – The Alternative Model of HKL

In this appendix, the MatLab script of the alternative model is found. This is the model used to simulate the HKL with the input from Stand 1 and Stand 2.

```
load zinterp;                          %Laster inn inpufilen
a=0.3;                                 %Tilegner verdi til a
strekk=zinp(:,5)+zinp(:,2);            %strekk=bpos+bitpos
strekk=strekk-min(strekk);             %Aktuell strekk (aktuell minus
                                       minste lengdden)
strekk=strekk/max(strekk);             %Normalisert strekk (aktuelle
                                       delt på største lengden)
b=0.65;                                %tilegner verdi til b
hastighet=zinp(:,6)/(max(zinp(:,6)));       %Normaliser hastig.

c=1-a-b;                                    % = 1
akseler=zinp(:,7)/(max(zinp(:,7)));         %Normalisert aksl.

modelhkl=a*strekk+b*hastighet+c*akseler;    %Summen av effeker

hookload=zinp(:,4)-min(zinp(:,4));          %faktisk HKL
hookload=hookload/max(hookload);            %Normalisert HKL

figure(4)
plot(zinp(:,1),hookload,'r',zinp(:,1),modelhkl)  %Plotteinstl.
legend('Measured HKL','Modeled HKL')             %Plotteinstl.
xlabel('Time (Seconds)')                         %Plotteinstl.
ylabel('Normalized HKL (-)')                     %Plotteinstl.
grid on                                          %Plotteinstl.
```

B – Interpolation Methods

This appendix includes the codes used to interpolate the measurements to be able to perform a higher resolution modeling and to try to catch the acceleration effect.

This first script, interpolation method 1, is the interpolation script used in the modeling of the alternative model for the Stand 1. The second script on the next page is a slightly improved one to smoothen the graphs. The latter one was used on Stand 2.

Interpolation Method 1

```
load hookldedv ;                                %modexa

zzz(:,1)=hookldedv(:,1)+hookldedv(:,2);     %min i sekunder
zzz(:,2)=hookldedv(:,3);
zzz(:,3)=hookldedv(:,4);
zzz(:,4)=hookldedv(:,8);
zinp(:,1)=zzz(1,1):0.01:zzz(end,1);
zinp(:,2)=pchip(zzz(:,1),zzz(:,2),zinp(:,1));
zinp(:,3)=pchip(zzz(:,1),zzz(:,3),zinp(:,1));
zinp(:,4)=pchip(zzz(:,1),zzz(:,4),zinp(:,1));
zzz(1:59,5)=zzz(1:59,3);
zzz([ 14 16 18 21 24 26 28  31 33 34 36 38 40 43],5)=nan;
%Fjerner samplingspuntkter (trappetrinn) nan=notanumber

zinp(:,5)=pchip(zzz(:,1),zzz(:,5),zinp(:,1));
   ble(1:59)=0;
   ble(59)=1;
   bl=~isnan(zzz(:,3));
   bld(1:59)=0;
   bld(2)=1;

velb=~isnan(zzz(:,5));     %isnan=kaster ut nan, beholder resten
hast=(diff(zzz(velb,5))./diff(zzz(velb,1)));      %hastighet
hasttid=(zzz(velb,1));     %indexverdier knyttet til hast.
hasttid=.5*(hasttid(1:(end-1))+hasttid(2:end));
%Legger hastigheten mellom (de opprinnelige) samplingspunktene

aksla=diff(hast)./diff(hasttid);
akslatid=.5*(hasttid(1:(end-1))+hasttid(2:end));

zinp(:,6)=pchip(hasttid,hast,zinp(:,1));
%Hastighet og tilhørende indexverdier (i tid) interpoleres
zinp(:,7)=pchip(akslatid,aksla,zinp(:,1));
%Akelerasjon og tilhørende indexverdier (i tid) interpoleres

return
```

Interpolation Method 2

```
load hookl20120615.txt ;

zzz(:,1)=(hookl20120615(:,1)-19)*60+hookl20120615(:,2);
zzz(:,2)=hookl20120615(:,3);
zzz(:,3)=hookl20120615(:,4);
zzz(:,4)=hookl20120615(:,8);
zinp(:,1)=zzz(1,1):0.01:zzz(end,1);
zinp(:,2)=pchip(zzz(:,1),zzz(:,2),zinp(:,1));
zinp(:,3)=pchip(zzz(:,1),zzz(:,3),zinp(:,1));
zinp(:,4)=pchip(zzz(:,1),zzz(:,4),zinp(:,1));

zzz(1:end,5)=zzz(1:end,3);
zzz(1:210,5)=zzz(211,3);  % Redigerer bort blokksenkning
zinp(:,5)=pchip(zzz(:,1),zzz(:,5),zinp(:,1));


mmm=20;          % Samplingssteg ved hastighetsberegning.Lenger
                 steg  gir mer glatting.

velb=~isnan(zzz(:,5));
hast=((zzz((1+mmm):end,5)-zzz(1:(end-mmm),5))./mmm*.2);
hasttid=(zzz(velb,1));
hasttid=.5*(hasttid(1:(end-mmm))+hasttid((1+mmm):end));


nnn=20            % Samplingssteg ved akselerasjons-
                  beregning.Lenger steg gir mer glatting.

  aksla=((hast((1+nnn):end)-hast(1:(end-
nnn)))./(hasttid((1+nnn):end)-hasttid(1:(end-nnn))));
akslatid=.5*(hasttid((1+nnn):end)+hasttid(1:(end-nnn)));


zinp(:,6)=pchip(hasttid,hast,zinp(:,1));
zinp(:,7)=pchip(akslatid,aksla,zinp(:,1));

return
```

C – RTDD of Stand 1 and Stand 2

This appendix presents the two stands picked out for modeling. Information about the pulling operation is given in the figure text.

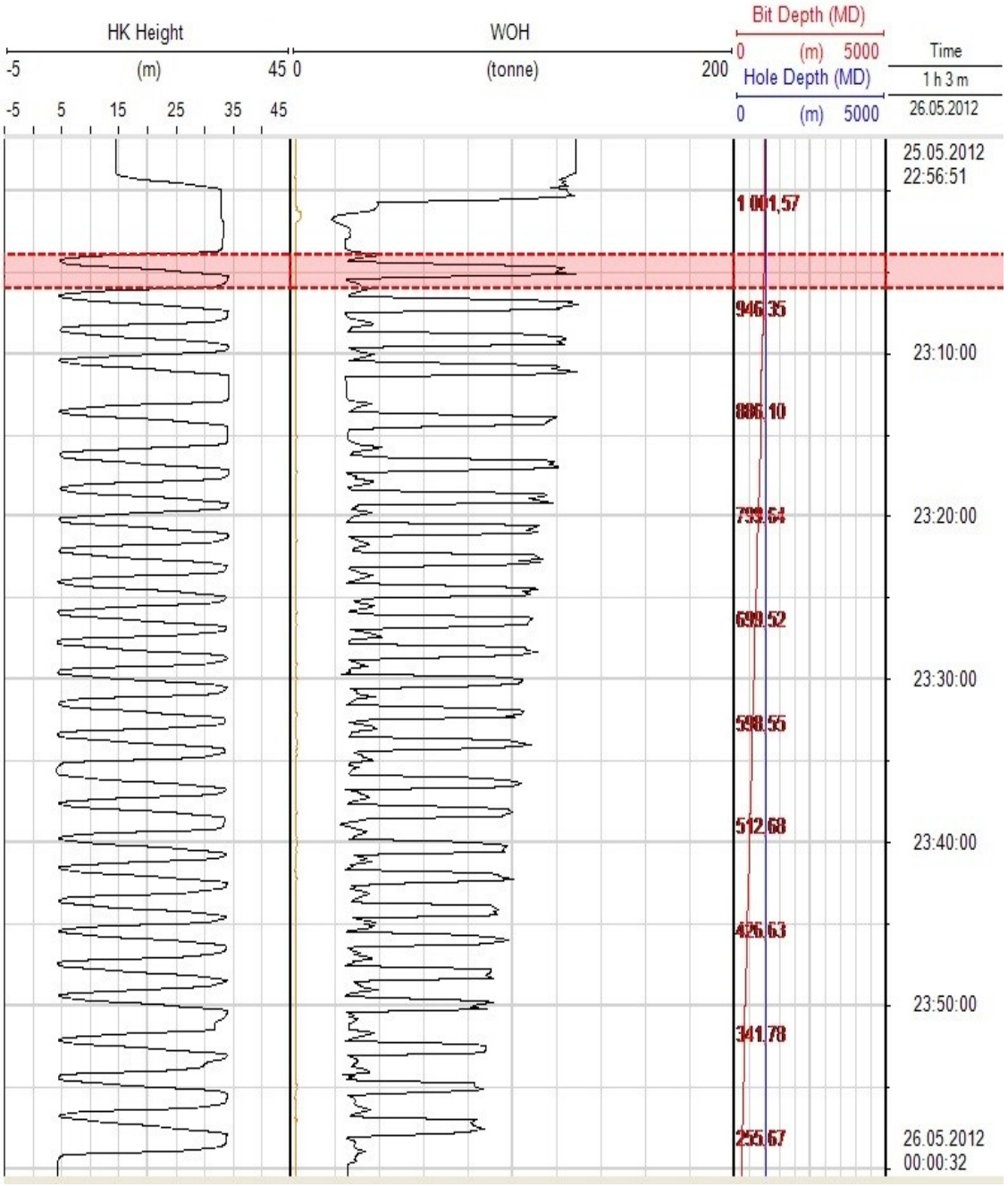

Figure 24: Tripping out operation. The 1 001,57 mMD long string is pulled out of a 1030 mMD long and 17 ½" wide hole. The selected area is the first stand to be picked out for modeling. A closer look at the specific stand can be found in to the left in Fig. 20. The transparent red area surrounded by a dotted rectangle in red is Stand 1.

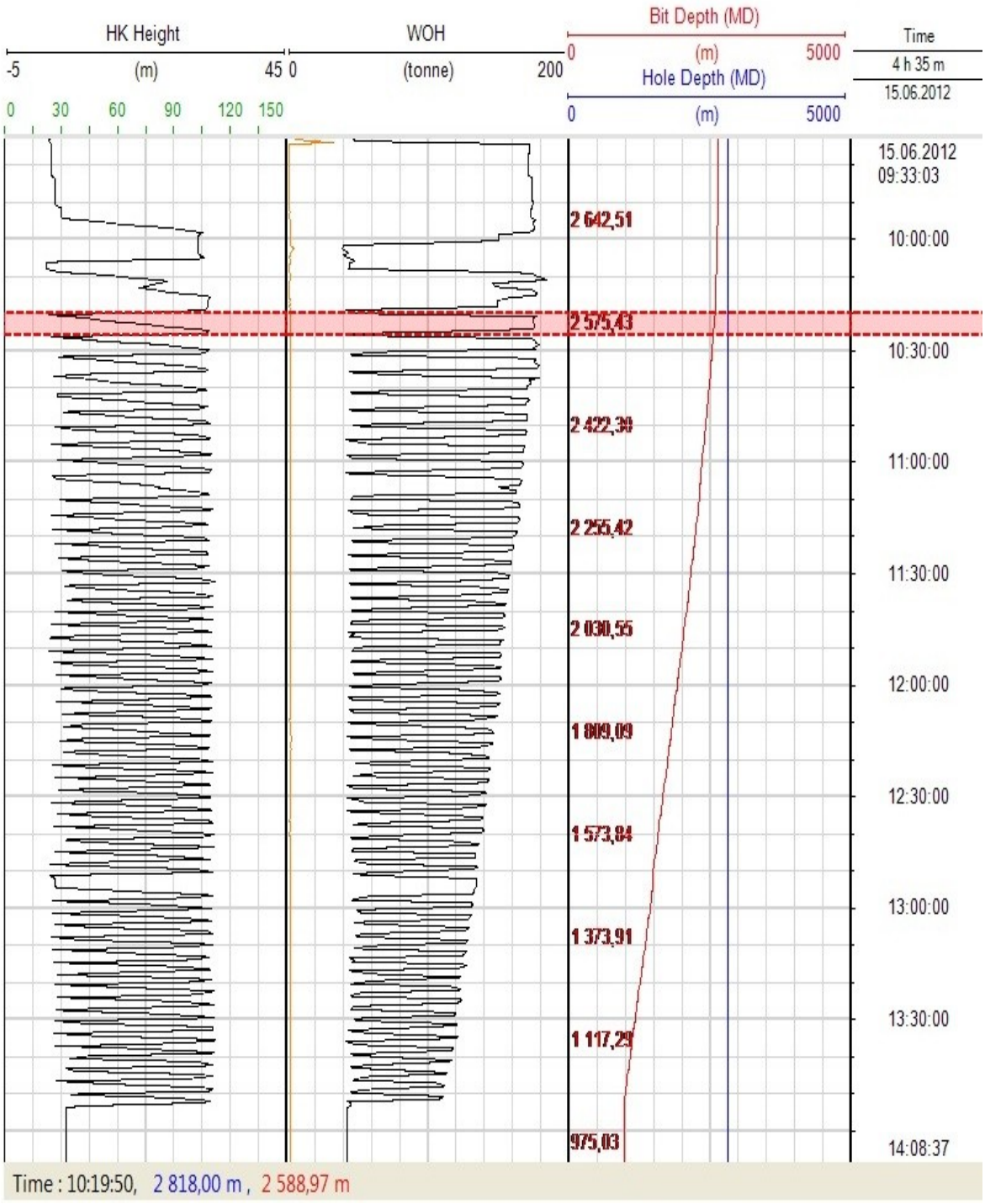

Figure 25: Tripping out operation of Stand 2. This figure shows the raw RTDD from the second well obtained from Discovery Web™, showing the start and main part of the tripping sequence of this 17 ½" section. A closer look at the specific stand can be found in to the right in Fig. 20. The transparent red area surrounded by a dotted rectangle in red is Stand 2.

D – The Mass Spring Model

This appendix contains the mathematical script used to run the mass – spring model and to obtain the results presented in the paper Mme et al. (2012), also shown in Fig. 19.

```
load modinterpol;
bha=75;                             %length of bha
pull=diff(modint(:,5,1));

L=modint(1,2,1)-Lbha;               %length of drillstring
clear modint;
load wellcoo                        %loads well coordinates

fprintf(1,'Hei\r')
M=5000;                             %number of timesteps  t represents
timesteps
%N=floor(21*L/4400);                %number of elements   n represents
element number
N=floor(41*L/4400);

deltat=.01;                         %timestep
E=2e11;                             %Youngs modulus for steel
rhoSteel=7800;                      %density of steel
densLSteelp=50;                     % Density per meter for steelpipe.
densLSteelbha=133;                  % Density per meter for bha.
A=densLSteelp/rhoSteel;             %cross section area of drillstring
m=L*densLSteelp/N;                  %mass of each element
mbha=Lbha*densLSteelbha;            %mass of bha
trest=1;
k=E*A/L*N*trest;                    %spring constant
g=9.8;                              %standard gravity
%REMG=0; %remove gravity (for debugging)
REMG=1;
st2kifr=2;%2;% static to kinematic friction ratio

alpha(1:M,1:N)=0;                   %angle of element N at timestep M
fr(1:M,1:N)=0;
fric(1:M,1:N)=0;
hgfr(1:M,1:N)=0;
hvfr(1:M,1:N)=0;
kvadr(1:M,1,N)=0;

ff=5.5;     %.1;%4nov<.2;%.04;%ff=0.01125;%.01; %25;  % Drag from mud

u(1,1:N)=uduakprosjektstatictest(L,N);

for n=1:N;u(1:M,n)=u(1,n);end

for n=1:N;
[vv8 ii8(n)]=min(abs(bp(3,:)-u(1,n)-L/N/2));
alpha(1,n)=atan2((-bp(1,ii8(n))+bp(1,(ii8(n)+10))),(-
bp(2,ii8(n))+bp(2,(ii8(n)+10))));
end;
%fprintf(1,'%5d',1)

for s=2:M;
t=s;
for n=1:N;
```

```
[vv8 ii8(n)]=min(abs(bp(3,:)-u(t,n)-L/N/2));
alpha(t,n)=atan2((-bp(1,ii8(n))+bp(1,(ii8(n)+10))),(-
bp(2,ii8(n))+bp(2,(ii8(n)+10))));
      end

fprintf(1,'\b\b\b\b\b%5d',s)       %  extrafr=5;
extrafr=1;
u(t,1)=u(t-1,1)+pull(s-1);
fricc=0.20;%0.15;   %friction coefficient, Âµ
%next line assigns frictional values
fric(t,N)=max(0,fricc*(k*(u(t,N)-u(t,N-1)-(u(1,N)-u(1,N-
1))).*sin(alpha(t,N)-alpha(t,N-1))+mbha*g*sin(alpha(t,N))));
fr(t,N)=extrafr*fric(t,N).*sign(u(t,N)-u(t-1,N));
hgfr(t,N)=fr(t,N);
kvadr(t,N)=abs(u(t,N)-u(t-1,N)       );
u(t+1,N)=k*deltat^2/mbha*((u(1,N)-u(1,N-1))-u(t,N)+u(t,N-1))+(2-
ff*kvadr(t,N))*u(t,N)-(1-ff*kvadr(t,N))*u(t-1,N)-
deltat^2/mbha*(fr(t,N))...
+REMG*deltat^2*g*(cos(alpha(t,N))-cos(alpha(1,N)));

      if ((((u(t,N))==u(t-1,N))&((k*deltat^2/mbha*((u(1,N)-u(1,N-1))-
u(t,N)+u(t,N-1))-REMG*deltat^2*g*(cos(alpha(t,N))-
cos(alpha(1,N))))<extrafr*deltat^2/mbha*st2kifr*(fric(t,N)))));
      u(t+1,N)=u(t,N);hvfr(t,N)=((k*deltat^2/mbha*((u(1,N)-u(1,N-1))-
u(t,N)+u(t,N-1))-REMG*deltat^2*g*(cos(alpha(t,N))-
cos(alpha(1,N)))))*mbha/deltat^2;hgfr(t,N)=hvfr(t,N);

      end;

for n=2:(N-1);
      fric(t,n)=max(0,fricc*(k*(u(t,n)-u(t,n-1)-(u(1,n)-u(1,n-
1))).*sin(alpha(t,n+1)-alpha(t,n))+m*g*sin(alpha(t,n))));
      fr(t,n)=fric(t,n).*sign(u(t,n)-u(t-1,n));
      hgfr(t,n)=fr(t,n);
      kvadr(t,n)=abs(u(t,n)-u(t-1,n)       );
      u(t+1,n)=k*deltat^2/m*(u(t,n+1)-2*u(t,n)+u(t,n-1)-(u(1,n+1)-
2*u(1,n)+u(1,n-1)))+(2-ff*kvadr(t,n))*u(t,n)-(1-ff*kvadr(t,n))*u(t-
1,n)-deltat^2/m*(fr(t,n))+REMG*deltat^2*g*(cos(alpha(t,n))-
cos(alpha(1,n)));
      %if (t==2&  n==40);pause;end
      %if n==9;display(strcat(['hvfr(' num2str(t) ',' num2str(9) ') =
' num2str(hvfr(t,9))])),end
      if (((u(t,n))==u(t-1,n))& ((k*deltat^2/m*(u(t,n+1)-
2*u(t,n)+u(t,n-1)-(u(1,n+1)-2*u(1,n)+u(1,n-1)))-
REMG*deltat^2*g*(cos(alpha(t,n))-
cos(alpha(1,n))))<deltat^2/m*st2kifr*(fric(t,n))));
      u(t+1,n)=u(t,n);hvfr(t,n)=((k*deltat^2/m*(u(t,n+1)-
2*u(t,n)+u(t,n-1)-(u(1,n+1)-2*u(1,n)+u(1,n-1)))-
REMG*deltat^2*g*(cos(alpha(t,n))-
cos(alpha(1,n)))))*m/deltat^2;hgfr(t,n)=hvfr(t,n);
      %if n==9;display(strcat(['hvfr('num2str(t) ',' num2str(9) ') = '
num2str(hvfr(t,9))])),end
      end;
      end;
      end

      u(t+1,1)=u(t,1)-pull(t);
```